UNIVERSITY OF OKLAHOMA

GRADUATE COLLEGE

ABRUPT AGRICULTURAL FLASH DROUGHT: AN INVESTIGATION OF RAPID DROUGHT DEVELOPMENT ACROSS VITAL AGRICULTURAL ZONES OF THE UNITED STATES

A THESIS

SUBMITTED TO THE GRADUATE FACULTY

in partial fulfillment of the requirements for the

Degree of

MASTER OF SCIENCE

By

BENJAMIN J. FELLMAN

Norman, Oklahoma

2023

ABRUPT AGRICULTURAL FLASH DROUGHT: AN INVESTIGATION OF RAPID DROUGHT DEVELOPMENT ACROSS VITAL AGRICULTURAL ZONES OF THE UNITED STATES

A THESIS APPROVED FOR THE
SCHOOL OF METEOROLOGY

BY THE COMMITTEE CONSISTING OF

Dr. Jeffrey Basara (Chair)

Dr. Jason Furtado

Dr. Thomas Galarneau

Acknowledgments

I would like to begin by thanking my advisor, Dr. Jeffrey Basara, along with my two committee members, Dr. Jason Furtado and Dr. Thomas Galarneau, for their guidance and feedback throughout this project. I have been extremely fortunate to have had such a supportive committee. In addition, I would like to thank my co-collaborators, Dr. Mari Tye and Dr. Jordan Christian. This project would not have been possible without your support, and I am grateful that I have had the opportunity to work closely with you both.

Moreover, I would like to thank my friends and family in Maryland and Pennsylvania. To my mom, dad, and brother, I want to thank you for motivating me to go to school for meteorology to pursue my dreams of studying the weather. With this, I also want to acknowledge all of my friends, professors, coaches and teammates from my undergraduate institution, Millersville University. The experiences I received during my education at Millersville in the classroom and on the tennis court provided me with the necessary support to be able to be successful in this field, and I will forever be thankful for those opportunities.

Lastly, I would like to thank all of my graduate school friends, my research team (CHEWe), and all others I have had the chance to meet and connect with during my time at the University of Oklahoma. One of the things I am most appreciative of within this field are the friendships and family-like support system we all have for one another. Without this support, I would not be where I am today and to that, I am eternally grateful.

This project was supported by the S3OK project within EPSCoR Oklahoma, funded by NSF Grant No. OIA-1946093. Thank you all for taking the time to read this document and learn more about my master's research.

Cheers bruv!

Table of Contents

List Of Tables

List Of Figures

Abstract

Flash droughts are highly impactful, sub-seasonal to seasonal events that pose a severe risk to agricultural production. The 2012 flash drought event in the United States is a prime example, as this event resulted in tens of billions of dollars of crop loss and caused longer-lasting effects to the overall US economy. This study examined impactful flash drought events across two agricultural regions of the central United States, spanning the 40-year period from 1981 to 2020. The two regions, the Southern Great Plains and Midwest, were selected given the agriculturally-dense areas in distinctively unique climate regions.

Using the standardized evaporative stress ratio (SESR), flash drought events were selected based on several factors, including the overall spatial coverage, rapid onset, and spread across the region. The events, defined as abrupt agricultural flash droughts (AAFDs), provide critical information regarding the timing of rapid drought transition across different areas of the United States and the implications they bring to agricultural producers. Initial results show that over the last 20 years, AAFDs have increased in frequency across critical regions of agricultural growth. Within the Southern Great Plains, essential findings within the timing of events illustrate how AAFDs, in conjunction with a winter La Niña pattern, led to a consistently below-average harvest of winter wheat the following growing season. Across the Midwest domain, results indicate a greater seasonality in AAFD events, with a majority of events transpiring during the late Spring and early Summer months.

Chapter 1

Introduction

Within the past 20 years, research efforts have increased on a newly defined phenomenon called flash drought. Flash drought was a term first introduced by Svoboda et al. (2002), to describe the rapid onset of drought conditions within just a few weeks. Compared to conventional drought events which occur on several months to year timescale, flash droughts are subseasonal to seasonal events (Pendergrass et al. 2020) that include land-surface interactions in addition to atmospheric processes. During flash drought events, there is an increased evaporative demand of the terrestrial surface due to factors including temperature, humidity, and wind speed (Svoboda et al. 2002; Peters et al. 2002; Anderson et al. 2011). Flash drought events rapidly desiccate the soil, leading to decreases in evapotranspiration and rapid aridification of the land surface within these regions (Hunt et al. 2014; Sánchez et al. 2016).

Initially, studies focused on defining key characteristics of flash drought events. Otkin et al. (2018) established two key characteristics of flash drought: (1) rapid intensification and (2) limited moisture/water availability in the surface. Further, a region must transition from non-drought characteristics to a state of drought by the culmination of the event. As a result, regions in drought-like states cannot undergo a flash drought event.

As a relatively understudied phenomenon (Lisonbee et al. 2021), several methods to detect flash drought were proposed using a variety of land-surface and atmospheric variables to identify the best metrics for event detection. Christian et al. (2019b) proposed a methodology using standardized evapotranspiration (ET) and potential evapotranspiration (PET) to calculate the standardized evaporative stress

ratio (SESR). This ratio provides a quantity that relates to the overall evaporative demand and moisture availability of the terrestrial surface at a point in time. Christian et al. (2021) applied SESR to 4 global datasets to identify global regions of enhanced flash drought events along with the evolution of temporal and spatial characteristics. These results showed a majority of the 15 worldwide regions used for the analysis have seen an increase in the overall occurrence of flash drought from 1980 to 2015. Other robust and reliable flash drought definitions have been proposed in literature. The standardized vegetation index (SVI) was one of the earliest metrics used to investigate flash droughts (Peters et al. 2002), as this index provided information regarding crop behavior during the 2000 Central United States flash drought. This method provided real-time information regarding degrading crop health conditions during this flash drought event and conveyed potential for being used to monitor changes in vegetation health. The evaporative stress index (ESI) has been used in several studies (Otkin et al. 2013, 2015; Nguyen et al. 2019), and is similar to SESR in that it uses evapotranspiration and potential evapotranspiration measurements from satellites to derive evaporative demand at the surface. The ESI methodology has been shown to provide early onset awareness to regions that may be beginning to experience rapid intensification into drought-like states. Additionally, the evaporative demand drought index, EDDI, (Hobbins et al. 2016; Pendergrass et al. 2020; Parker et al. 2021) has been used as an effective tool for capturing flash droughts and their understanding of this subseasonal to seasonal phenomenon. Lastly, several studies have also used the United States Drought Monitor categorical breakdowns as a metric to detect when rapid intensification is ongoing in regions. Ford et al. (2015) proposed using this drought monitoring system to distinguish varying intensities of drought events, noting specific categorical thresholds that must be surpassed within a specific temporal window to be quantified as a flash drought event. Their study set the threshold that for an event to be considered a flash drought, a region must see a 3-category increase

in drought severity within an 8-week window. Pendergrass et al. (2020) proposed a shorter duration definition, stating flash drought identification is reached for regions that see a 2-category increase in drought severity within a 2-week window.

In addition to developing metrics to define these events, several studies have proposed categorizations for flash drought events. For example, Mo and Lettenmaier (2016); Koster et al. (2019); Li et al. (2020); Mo and Lettenmaier (2020) developed methodologies to describe two main types of flash drought events: precipitation-deficit and heat wave flash droughts. Precipitation-deficit flash droughts are classified as events more directly caused by a significant lack of precipitation. Within the definition of precipitation deficit flash droughts, precipitation must fall to a minimum during the onset of the event (Mo and Lettenmaier 2020). Heat wave flash droughts are induced by a sustained period of enhanced temperature anomalies which results in increased evaporative stress on the ground and decreased water availability. These studies have provided significant insight into the main drivers behind flash droughts on regional scales in many hotspot locations, including the United States and the Yellow River Basin in China. Mo and Lettenmaier (2020) found that across the United States, precipitation deficit flash droughts are more commonly seen across regions of the South, specifically the Southern Great Plains. Moreover, heatwave flash droughts were more commonly seen in areas further north, with a maximum of events recorded in regions of the Midwest and Ohio Valley.

With the development of methodologies to identify and classify flash drought, research focused on major flash drought events to understand the processes and impacts of these events. One of the earliest studies of rapid drought evolution included an investigation of the 1988 North America Drought, a rapidly developing event that occurred during the summer months. This rapid transition into drought was driven by a quasi-stationary ridging pattern that set up across the central United States (Trenberth and Branstator 1992). While studies did not define this event as a flash drought,

it was shown to be a rapidly evolving drought and displayed several characteristics of flash drought behavior. This event caused several major impacts, including restricting flow on the Mississippi river during the months of June and July, resulting in billions of dollars of loss within the barge industry (Changnon 1989). The 2012 flash drought event was an impactful and disastrous event for agricultural producers, resulting in tens of billions of dollars in damage to crops (Rippey 2015). From May to August 2012, temperature anomalies exceeding one standard deviation above climatology and precipitation anomalies at least one standard deviation below climatology occurred across the central United States (Hoerling et al. 2014). This sustained period of anomalously warm temperatures, along with below-average precipitation concerning climatology, enhanced the evaporative demand of the environment across the central United States, leading to a rapidly developing flash drought encompassing millions of square kilometers (Basara et al. 2019). Many regions across the central United States recorded average soil moisture values below the 10th percentile during this temporal window (Hoerling et al. 2014). Given the timing of this event concerning the growing season of crops, such as corn, the flash drought event stunted agricultural growth in several regions, resulting in severe losses for agricultural producers (Basara et al. 2013).

Other flash drought events within the 21st century have caused significant impacts on agricultural regions. Just two years before the 2012 event, an expansive flash drought evolved over portions of Russia during the summer of 2010, disrupting the world economy. This event occurred over an agriculturally dense region of the country, causing severe impacts on the yield of winter and spring wheat by 30 to 80 percent (Hunt et al. 2021). Wheat yields were so low that an export ban was posed following this event (Christian et al. 2020). In 2017, the Northern Great Plains' flash drought resulted in severe consequences. Within three months, regions of Montana and the Dakotas went from non-drought states to exceptional drought, the most severe category listed within the U.S. Drought Monitor (He et al. 2019). This event resulted

in billions of dollars of crop loss, causing significant impacts to agricultural producers (Hoell et al. 2020). Flash drought events have repeatedly caused billion-dollar losses to agricultural producers, resulting in severe hardships for these stakeholders and the overall economy.

While several case studies have analyzed the impacts of a single flash drought event over an agricultural region, few have examined whether the same region has experienced multiple flash droughts during the observational record. Events such as the 2010 Russian flash drought and the 2012 and 2017 United States flash droughts demonstrate the catastrophic impacts these events pose to agricultural producers, as the timing, duration, and strength of these events have been shown to cause serious problems to overall crop yield. In addition, these events convey how the timing of flash droughts has significant impacts on the yield of crops based on their growing season. For example, the 2012 flash drought event across the United States extended into portions of the Southern Great Plains that are heavily used as agricultural land for winter wheat. However, because this event occurred during the end of the growing season/harvest for winter wheat, the yields seen from this crop were not as heavily impacted (USDA, Economic Research Service 2015). A research gap includes fundamental understanding of how flash drought event frequency, timing, and impacts have changed across agricultural regions. Because crop development is dependent on atmospheric conditions including temperature, precipitation, and sunshine amongst other factors (Sacks et al. 2010; Eck et al. 2020; dos Santos et al. 2022), flash drought events have serious potential to enhance atmospheric conditions that are unhealthy for crops. Moreover, depending on the timing of flash drought events, one crop type may experience more impacts compared to others because of the distinct growing seasons of crops. As such, this study examines the frequency, spatial extent, and atmospheric drivers of flash droughts in the Southern Great Plains and Midwest regions with specific focus on abrupt agricultural flash drought (AAFD) events and the associated impacts following these events. To begin, initial results convey that

flash drought remains a highly variable event spatially, even amongst climate regions of the United States. The timing of flash drought onset also indicates the potential ramifications this phenomenon could pose to stakeholders and agricultural producers in both regions. The results indicate that further refinements to flash droughts can be identified with respect to their abrupt spatial onset across a large proportion of the region under analysis. The definition of abrupt agricultural flash drought (AAFD) events will be further elaborated on below.

Chapter 2

Date and Methods

2.1 Reanalysis and Crop Datasets

Several reanalysis variables were used to examine the impacts flash drought events pose to crops in both regions. To begin, three ERA5 datasets of reanalysis data were used. These datasets included daily averaged ET, PET, and soil moisture. ET, PET, and soil moisture datasets were analyzed from 1981-2020. ERA5 ET and PET reanalysis data is used for the identification of flash drought across both domains (Hersbach et al. 2020). Soil moisture data was used as a second parameter to assess surface soil moisture responses during and after flash drought events. Within the soil moisture data, this study analyzed the top layer of soil moisture, measuring to a soil depth of 7 centimeters. Although long-term droughts can cause a significant impact to deep-layered soil moisture, soil moisture in the shallowest layers provides a better method for monitoring short-term droughts (Xu et al. 2021).

Further, in the results section, the role of the El Niño Southern Oscillation (ENSO) and its impact on abrupt flash drought events will be examined. To do so, the Oceanic Niño Index (ONI) was used to determine the regime of ENSO at a point in time. ONI (Trenberth and Stepaniak 2001) incorporates a 3-month running mean of sea surface temperature (SST) anomalies within the Niño 3.4 region, defined by 5°S-5°N, 120°-170° W. This region was selected as Trenberth (1997) determined Niño 3.4 is the critical region of ocean-atmospheric interactions which regulate the teleconnection. Moreover, studies including Flanagan et al. (2019) demonstrate sea surface temperatures in this region of the Pacific Ocean are influential in driving circulation patterns

which can lead to enhanced precipitation regimes across portions of the United States, including the Southern Great Plains. As a result, ONI data from the Climate Prediction Center (CPC) was implemented to determine the regime of ENSO at any time during the study window.

Lastly, surveyed crop yields and crop condition reports were used for this study. For the analysis of the Southern Great Plains, surveyed total crop yields of winter wheat were examined by the United States Department of Agriculture, National Agricultural Statistics Survey (USDA, NASS) yearly from 1981 to 2020 across Kansas, Texas, and Oklahoma. Moreover, weekly crop condition reports of winter wheat were also analyzed to determine the progression of winter wheat throughout various points of the growing season. Within the Midwest domain, surveyed crop yields of corn and soybeans in Iowa were analyzed from 1981 to 2020. Crop conditions of corn and soybeans within the state were also examined for 2003 to convey the impacts that a flash drought event had on these crops. Crop conditions and yields are assessed through producers, agribusinesses, and traders each week through several modes of communication, including a secured internet site, questionnaires, and by phone (Vogel et al. 1999). In all weekly crop condition reports, crop conditions can fall into one of five categorical conditions. Figure 2.1 lists all categorizations of crop yields and their significance to what is expected in overall yields for the crop. Crops listed as "good" indicate that field prospects are average, and any crops listed in "excellent" condition indicate that yield prospects are expected to be above average. Crops grouped into the other three categories, "fair,"; "poor,"; or "very poor," are expected to have some variation of crop loss. Crops listed as "very poor" indicate the potential for extreme to total yield loss expected.

Excellent	Good	Fair	Poor	Very Poor
Yield prospects are above normal .Crops are experiencing little or no stress.	Yield prospects are normal. Mositure levels are adequate and disease, insect damage, and weed pressures are minor.	Less than normal crop condition. Yield loss is a possibility but the extent is unknown.	Heavy degree of los to ield potential which can be caused by excess soil moisture, drought, or disease.	Extreme degree of loss to yield potential, complete or near crop failture. Pastures provides very little or no feed.

Figure 2.1: Categorizations of crop conditions designated by the USDA NASS.

2.2 Defining Critical Agricultural Zones

The motivation for this research stems from several studies (Peters et al. 2002; Basara et al. 2019; Christian et al. 2020; Hoell et al. 2020; Hunt et al. 2021) which focused on significant flash drought events that evolved across agricultural regions. Each flash drought event had major impacts on agricultural producers and economic losses as crop health and yields suffered. Although past studies have investigated regional characteristics of flash drought across the United States (Christian et al. 2019a), this study examined how flash drought varies on smaller spatial scales specifically linked to high agriculture production zones.

A major goal of this study was to select regions within the United States that are similar in geographic location yet situated in unique climate zones. While selecting regions, planting maps from the USDA were used to validate the most concentrated regions of crop use in the United States. Two regions of investigation were selected for this analysis. The first study domain over the Southern Great Plains (Figure 2.3), encompassing the region from the New Mexico/Texas border into central Oklahoma and much of Kansas, is an essential provider of winter wheat in the United States. Figure 2.2 illustrates the concentrations of winter wheat crops in the United States, with the highest crop densities indicated by the darker green shades. Winter wheat is of additional interest to investigate, given the impacts this crop faced during the 2010 Russian flash drought event (Hunt et al. 2021). Moreover, studies such as Zhao et al. (2022) have shown that specific atmospheric conditions seen in flash droughts can pose increased impacts on winter wheat health in the United States. In particular, Zhao et al. (2022) illustrated that hot, dry, and windy events pose a severe risk to winter wheat crop health during the heading-to-maturity phase of the winter wheat growing season.

The second region encompasses all of Iowa and several surrounding states, including northern Illinois and southern Wisconsin (Fig. 2.3). This region is agriculturally

important for several crops, including soybeans and corn; Figure 2.2 also illustrates concentrations of these crops planted across the United States, indicating millions of acres of soybeans and corn are planted annually within the Midwest. Both of these crops have been impacted by previous flash drought events, such as the 2012 flash drought across the central United States (Basara et al. 2013; Jin et al. 2019). Nonetheless, other smaller-scale flash drought events likely have significantly impacted crop health and yields. Quantifying and defining all flash drought events will help identify the characteristic behavior and impacts of these events.

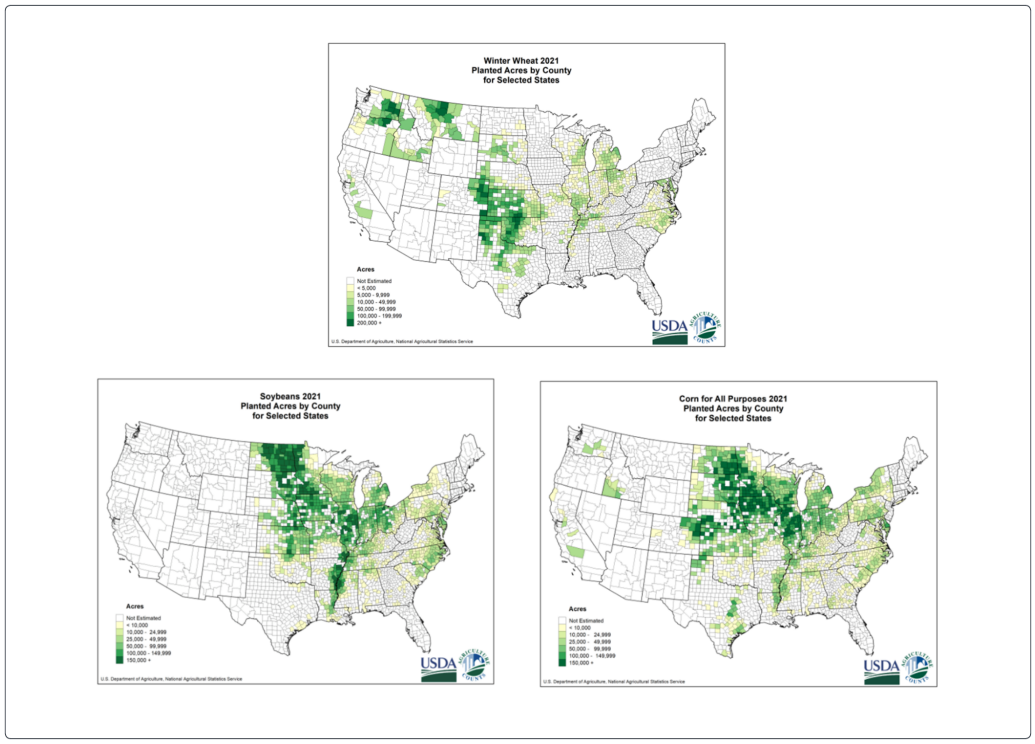

Figure 2.2: Planted crop acres for winter wheat (left), soybeans (bottom left), and corn (bottom right) in 2021.

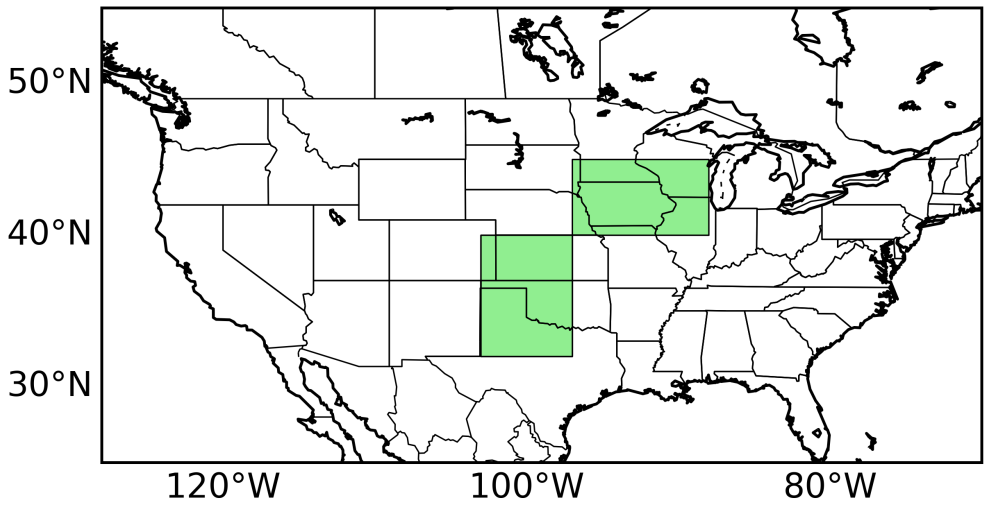

Figure 2.3: Visual representation of the critical agricultural zones selected for investigation. The Southern Great Plains (SGP) domain is bounded by 32°- 40° N, 103°- 97° W. The Midwest (MW) domain is bounded by 40°- 45° N, 97° - 88° W.

2.3 Flash Drought Identification using SESR

Flash drought events were detected using a modified framework for SESR from Christian et al. (2019b) and described in Christian et al. (2022). This methodology uses ET and PET to calculate the evaporative stress ratio (ESR). ESR is a ratio of ET to PET at one point in time and is calculated via the equation:

$$\mathrm{ESR} = \frac{\mathrm{ET}}{\mathrm{PET}}$$

Evapotranspiration describes the amount of water being evaporated into the environment from the surface as a function of temperature, relative humidity, and wind speed (Pereira et al. 1999). Potential evapotranspiration reflects the expected amount of water that should be evaporated into the environment based on the ambient atmospheric conditions (Granger 1989). Potential evapotranspiration (commonly referred to as ET_0) is derived via the United Nations Food and Agriculture Organization (FAO) Penman-Monteith approximation (Allen et al. 1998):

$$\mathrm{ET}_0 = \frac{0.408\Delta(\mathrm{R_n} - \mathrm{G}) + \gamma\frac{900}{\mathrm{T}+273}\mathrm{u}_2(\mathrm{e_s} - \mathrm{e_a})}{\Delta + \gamma(1 + 0.34\mathrm{u}_2)}$$

Within this equation, Rn is net radiation at the crop surface, G is soil heat flux density, T is the mean 2-meter daily air temperature, (e_s - e_a) represents the saturation vapor pressure deficit, U_2 is the 2-meter wind speed, Δ represents the rate of change of saturation specific humidity with air temperature, and γ is the psychrometric constant. The FAO Penman-Monteith approximation has previously been used in literature to evaluate PET across agricultural regions (Sentelhas et al. 2010).

During flash drought events, ET significantly decreases as a result of decreasing soil moisture availability. On the contrary, PET remains constant or even increases as a result of increased temperatures as well as decreased atmospheric humidity during flash droughts (Christian et al. 2020; Hoerling et al. 2014). Both of these factors

result in a decreasing ESR in time (Christian et al. 2019a) and the higher evaporative demand results in rapid soil moisture loss.

For this study, ERA5 reanalysis data of daily ET and PET were used for the period spanning 1981 to 2020 to identify flash drought events. Further, the events were restricted to the agricultural growing season, extending from March to October. This is fairly consistent with previous studies that have investigated flash drought during the growing season (Christian et al. 2019a, 2021). The months of March and October were included in the defined growing season given crops being investigated in this study have major growing stages during these months of the year. For this study, events that started before March but extended into the growing season for at least one pentad in time were included. Moreover, events that began rapid intensification before the end of October were also included. Both datasets have a 0.25 x 0.25-degree grid spacing, encompassing a spatial domain of 30 x 30 kilometers per grid point.

A limitation of using the ESR is that daily ET and PET values can fluctuate significantly. Christian et al. (2019b) utilized pentads, or 5-day periods, during flash drought events to better capture these changes in ESR. As such, daily ESR was converted into averaged pentads, then standardized at each grid point for each pentad in time, using the climatological average from the study period. This final step produces the standardized evaporative stress ratio (SESR). SESR values are calculated into percentiles and used in the methodology for detecting flash drought events. Fig A 2.1, taken from Christian et al. (2019b), provides a flow chart depicting the calculation of SESR for this study.

The change in SESR between each pentad was also calculated using the same process described above. Because the change in SESR values were standardized, they can also be expressed and evaluated as percentiles. Thus, the standardized change in SESR identifies how rapidly SESR values change between two pentads compared to climatology. These percentiles were also used to analyze and calculate flash drought

events. Finally, the Savitzky-Golay filter was applied to the SESR and the change in SESR between pentads. This technique has been previously used in smoothing data for other land-surface variables including the Normalized Difference Vegetation Index (NDVI) and satellite-based Land Surface Water Index (LSWI) (Chen et al. 2004; Christian et al. 2022). With a total window length of 21 pentads, or 105 days, this metric smooths the data to better represent the subseasonal-to-seasonal changes of SESR.

This methodology was defined to capture drought events that rapidly developed and intensified on a subseasonal-to-seasonal timescale. The three criteria used to detect flash drought occurrence through SESR and the change in SESR are as follows:

1. The change in SESR over a flash drought event between each pentad is below the 25th percentile.

2. SESR is less than the 20th percentile at the duration of the event.

3. Flash drought length is longer than 30 days (6 pentads).

The first criterion analyzes the pentad to pentad change in SESR. The 50th percentile of the change in SESR equates to the climatological average change in SESR values between 2 pentads of time. Therefore, values of the change in SESR between two pentads that fall below the 25th percentile reflect that SESR values are decreasing at a rate that exemplifies a rapid transition event compared with climatology. Values must remain below this threshold throughout the entire event, signifying that rapid drought transition is ongoing through all pentads of the event. The second criterion requires the environment to reach drought status during rapid intensification; the requirement of SESR being less than the 20th percentile signifies that the SESR percentiles have surpassed the drought threshold. Furthermore, this criterion

solidifies that regions must not have previously been in drought before flash drought occurs. The third criterion focuses on flash drought occurring within a subseasonal-to-seasonal temporal window. It ensures that an event's duration must be at least 30 days long. With a defined methodology for detecting flash drought events, preliminary analysis of flash drought over these regions could begin.

2.4 Defining Abrupt Agricultural Flash Droughts (AAFDs)

Flash drought events differ in their spatial propagation over time. Figures 2.4a and 2.4b display the time series of flash drought from 2 years within the Southern Great Plains domain and highlight the percentage of grid points with flash drought initiation during a pentad in time. While the flash drought identification was met for almost half the domain during 2007 (Fig. 2.4a), it began at very different periods in time over several months. Assessment of the same time series analysis for 2003 conveyed significant differences in the temporal evolution compared to 2007. Figure 2.4b displays that flash drought initiation during 2003 occurred simultaneously across a significant portion of the observed region at one point in time. During this event over the summer, nearly all grid points began rapid drought transition within a three-pentad, or roughly two-week, window in June. Events such as the 2010 Russian flash drought displayed very similar characteristics whereby the timing of flash drought initiation occurred nearly simultaneously (Christian et al. 2020). Moreover, additional studies have found that flash drought onset is occurring more rapidly in time (Qing et al. 2022).

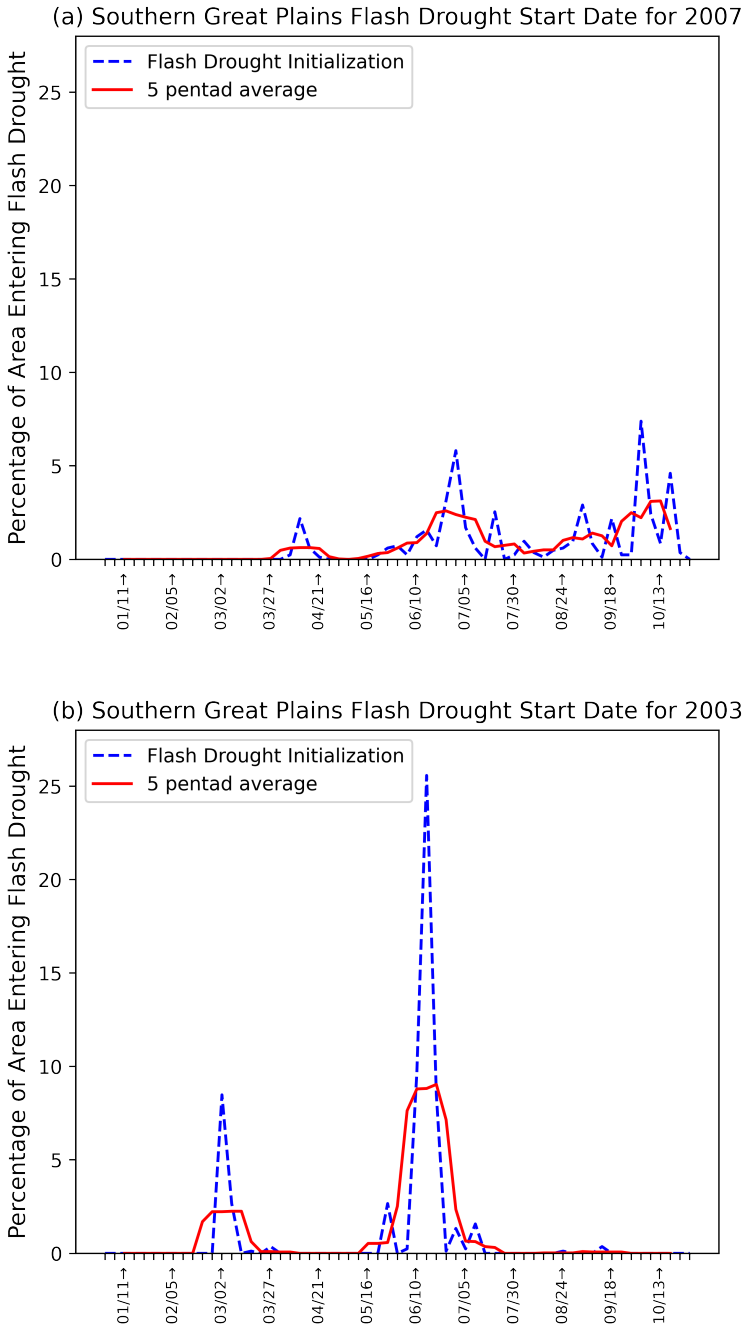

Figure 2.4: (a) Time series of the percentage of grid points that entered flash drought criteria at a pentad in time in the Southern Great Plains domain during the year 2007. The blue dashed line represents the raw data over each pentad, and the red line marks a five-pentad running average using a centered difference approximation. (b) Same as (a), but for the year 2003.

As a result, this study will specifically focus on flash drought events that overspread an agricultural region at similar pentads in time. Given drought affects the decision-making process for crops such as winter wheat (Klemm and McPherson 2018) and affects the yields of winter wheat, corn, and soybeans across the study domains (Mauget and Upchurch 1999; Zipper et al. 2016), it was of interest to define these impactful episodes of rapid drought development. This subset of events is defined as abrupt agricultural flash droughts (AAFDs); AAFDs describe a rapidly intensifying drought simultaneously occurring across a domain with intensive agriculture. To evaluate AAFD events across each study region which encompasses hundreds of thousands of square kilometers of land with heavy agricultural usage, this study proposes a methodology for identification with several vital criteria. These criteria focus on three key event characteristics:

1. A peak of flash drought initiation across the region at one-time step. Within this criterion, a consistent aerial region enters flash drought at the same time. The peak is defined as Pentad 0, marking this study's beginning of an AAFD event.

2. Secondly, within a defined temporal window from Pentad 0, a defined area must transition into rapid intensification.

3. Flash drought initiation must decrease beyond the temporal window encapsulated by Criteria 1 and 2. As such, this ensures that the defined area abruptly transitions to flash drought at approximately the same time.

Based on the above criteria, sensitivity testing was conducted using four permutations of contrasting spatial thresholds and temporal window of investigations over both regions. Each permutation evaluated abrupt flash drought episodes over the

40 year data set in order to analyze the frequency and timing of events across both regions. The permutations and their associated combinations of spatial and temporal thresholds (Figure 2.5) were tested for their sensitivity and to select a final definition for AAFD events. Figures 2.6 and 2.7 illustrate the results of the sensitivity testing across the Southern Great Plains and Midwest domains, respectively.

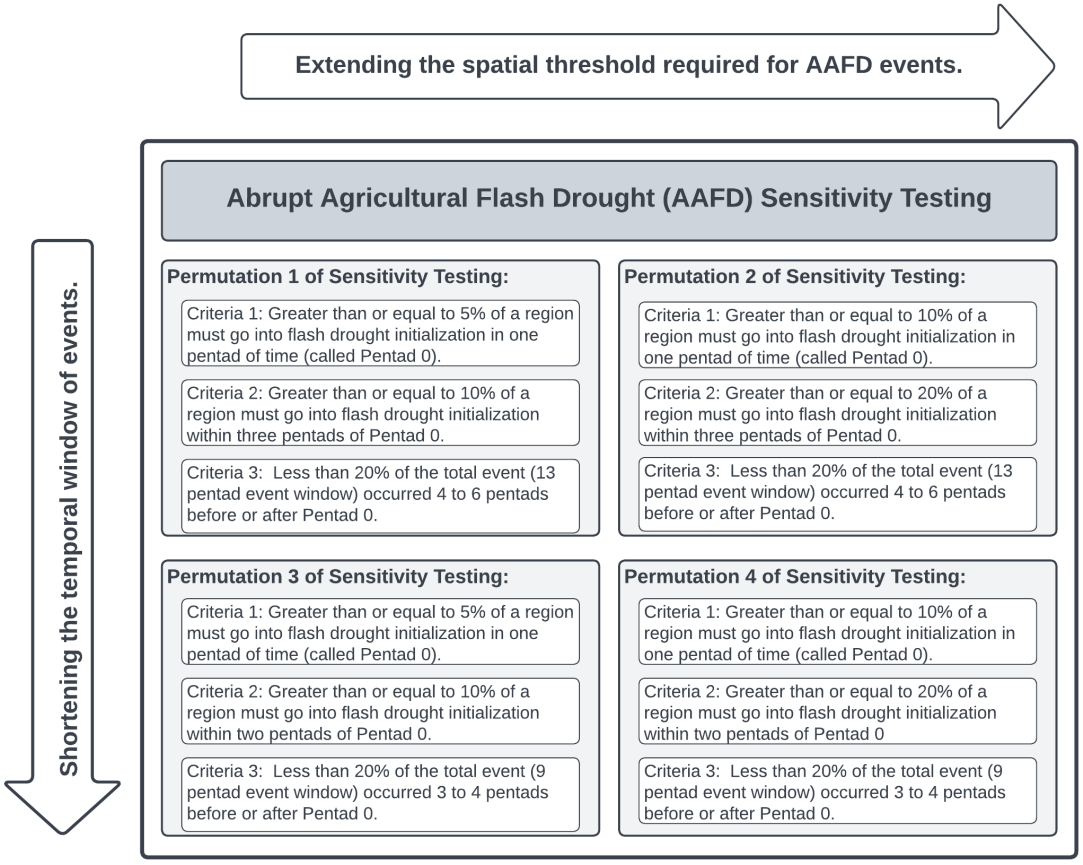

Figure 2.5: Illustration of the 4 permutations of sensitivity testing performed over both regions to determine AAFD events from 1981 to 2020. Events collected must have occurred over some part of the growing season, defined from March to October.

Beginning with the Southern Great Plains region, the initial sensitivity test outlined in Permutation 1 yielded 40 AAFD cases over the 40-year period. During several of these years, multiple abrupt flash drought events occurred under these criteria. The

analysis only accounted for the first flash drought occurrence over an area, thus subsequent events occurred over different land areas that did not already surpass flash drought identification during the year.

While each of the permutations used a slightly modified methodology, the results varied considerably, providing more explicit guidance for the finalized AAFD definition. Permutation 2 retained the same temporal window criterion as Permutation 1. However, expanding the spatial threshold criterion resulted in a decrease in recorded events, as only 15 were recorded within this test. While Permutation 3 had a shorter temporal window compared to Permutation 1 and retained the same spatial threshold, the number of cases remained very similar (36 AAFD events). Permutation 4 had the same spatial threshold as Permutation 2, and temporal threshold as Permutation 3, and yielded a similar AAFD frequency to Permutation 2 (14 AAFD events). These results indicate that changes to the spatial threshold in Criteria 1 and 2 across the Southern Great Plains region were more influential to changing the frequency of AAFD events yielded in comparison to changing the temporal window in identifying AAFD cases.

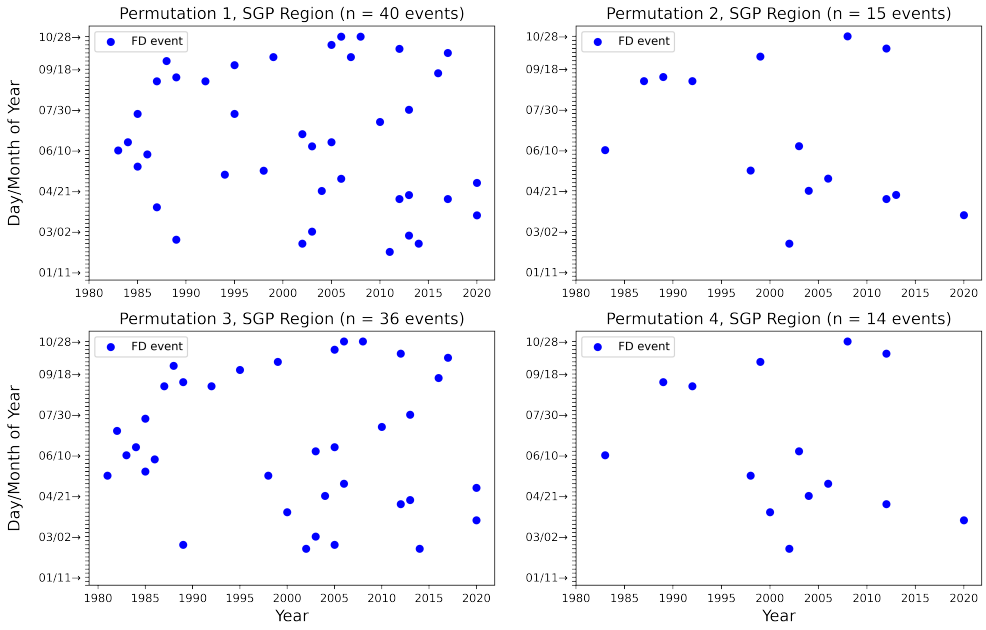

Figure 2.6: Results of sensitivity testing across the Southern Great Plains domain.

Similar results were found for the Midwest region. Within Permutation 1, 42 AAFD events were recorded over the period. The year 2007 featured four separate AAFD events. Like the Southern Great Plains region, the AAFD events recorded in Permutation 2 across the Midwest decreased by more than half compared to Permutation 1 (17 events). Permutation 3 yielded nearly the same number of events as Permutation 1 (37 events), and Permutation 4 yielded 14 events, a slight decrease from the number recorded in Permutation 2.

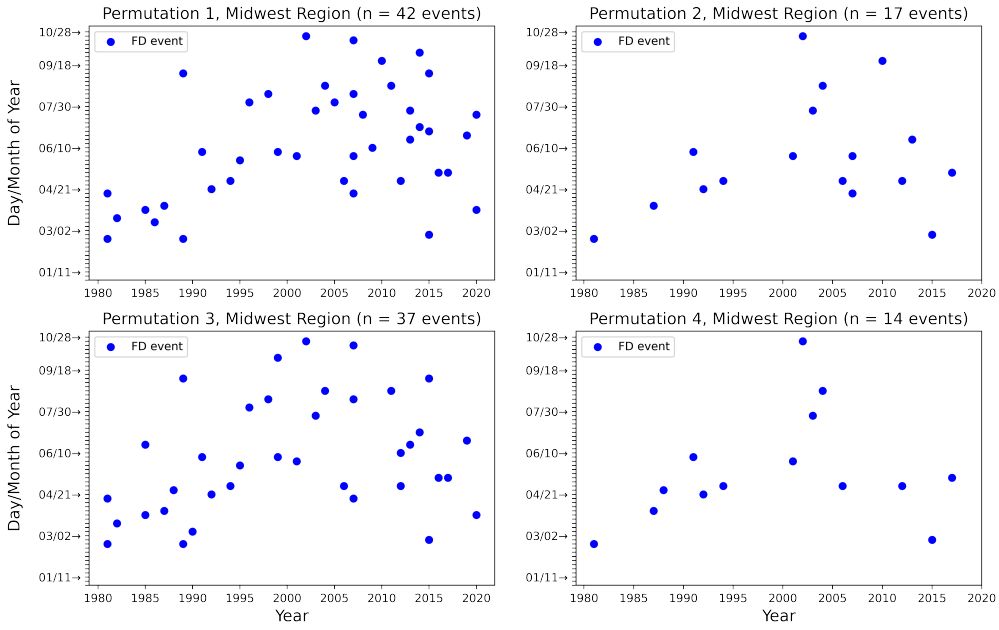

Figure 2.7: Same as Figure 2.6, except for the Midwest domain.

From these results, it is noted across both regions that expanding the spatial threshold for consideration decreases the number of AAFD events. However, shrinking the temporal investigation window for abrupt events slightly decreases the caseload and better discriminates against flash drought events from being classified as abrupt or not. Given that these events occur spontaneously and rapidly increase in spatial coverage, a smaller temporal window best fits the flash drought events captured in this study. Thus, the proposed definition of AAFD events in this research uses the temporal window of Cases 3 and 4, consisting of a 9-pentad, or 45-day, total window.

Rather than relying on a variable percentile-based spatial threshold, a common spatial definition to identify flash drought events would be preferable for both regions. The Secretarial drought declarations posted by the USDA highlight spatial regions that require government assistance due to drought-driven issues in any given year. The 2020 map (Figure 2.8) shows that aside from the comprehensive and ongoing southwest drought, several smaller areas on the east coast and central United

States required some form of government assistance following drought conditions in 2020. This also included a region across the Midwest covering tens of thousands of square miles which requested disaster resistance. From initial analysis, it was found that flash drought activity occurred over much of this region in 2020 (Figure 2.8), signifying that rapidly intensifying drought events can pose severe consequences to affected regions. Moreover, it indicates that small-scale regions which undergo rapid drought development can experience significant impacts that must be accounted for. Ultimately, this helped guide the spatial threshold being defined for the methodology of these events, given it affected a major agricultural zone.

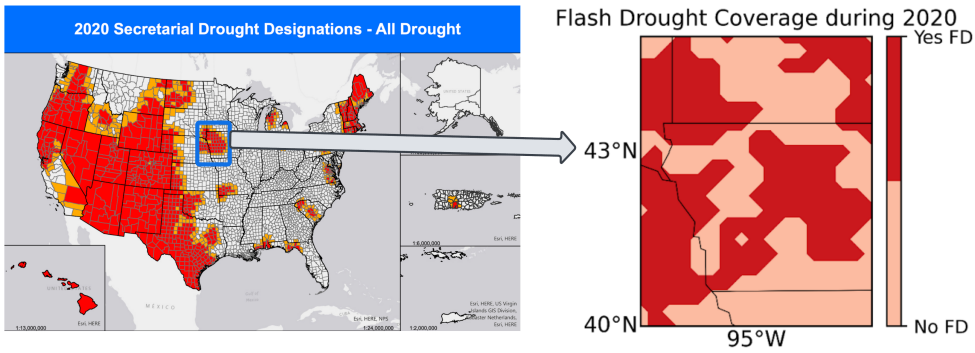

Figure 2.8: 2020 Secretarial Drought Designation Map illustrating counties of the United States that required secretarial assistance due to drought conditions during the year 2020 (USDA, Farm Service Agency 2020). The second diagram depicts the affected region in the Midwest and illustrates which portions of the domain underwent flash drought development in 2020.

Drawing from the sensitivity testing and adopting common spatial thresholds across regions gives the final definition for abrupt agricultural flash droughts, as seen in Figures 2.9 and 2.10:

1. 37,500 square kilometers ($\sim$ 15,000 square miles) must enter flash drought transition at one pentad. This time step is referenced throughout this study at 'Pentad 0' of an AAFD.

2. 75,000 square kilometers ($\sim$ 30,000 square miles) must enter flash drought transition within two pentads from this peak, Pentad 0, mentioned in Criterion 1.

3. 20% or less of flash drought identification begins at the end periods of the 9-pentad window of these events. The end periods include 3 to 4 pentads before and after this peak of initialization, defined as Pentad 0.

Figure 2.9 illustrates a flow chart diagram to distinguish the classification of AAFD events. Furthermore, Figure 2.10 provides a depiction of an AAFD event over the Midwest region in 1987 to provide a visual representation of the temporal window being used for AAFD analysis within each criterion. Criteria 1 and 2 focus on defining events that encompass a broad area of land and likely have tangible impacts (e.g., Federal drought declarations). Criterion 1 focuses on ensuring an event has a clear starting point associated with the region entering into drought. The spatial thresholds for Criteria 1 and 2 were selected using Figure 2.8 as a reference. As described above, in 2020, a small area of western Iowa and eastern Nebraska needed governmental assistance due to drought affecting these regions. This area, roughly covering 20 to 30 thousand square miles, was used as a baseline measurement for the spatial extent in Criterion 2, given that much of the area underwent rapid drought intensification. Regarding the spatial properties in Criteria 1 and 2, it was chosen that the flash drought coverage in these areas can, but does not have to, be continuous in space to surpass the thresholds set. Given the Secretarial drought designation maps

shown in Figure 2.8, it is evident that isolated regions within a state may require additional assistance due to localized drought impacts. Thus, enforcing a continuous spatial domain within the criteria would likely neglect some flash drought events which could be severe enough to pose impacts. Lastly, Criterion 3 constrains the event coverage to be maximized within the 5-pentad window defined in Criterion 2. The 20% benchmark was consistently used throughout each case of sensitivity testing and within the final definition as this value is continuously used within this study as a defined lower bound. Thus, to keep in continuity with the study, this value was set and ensures events have a core window of major flash drought development.

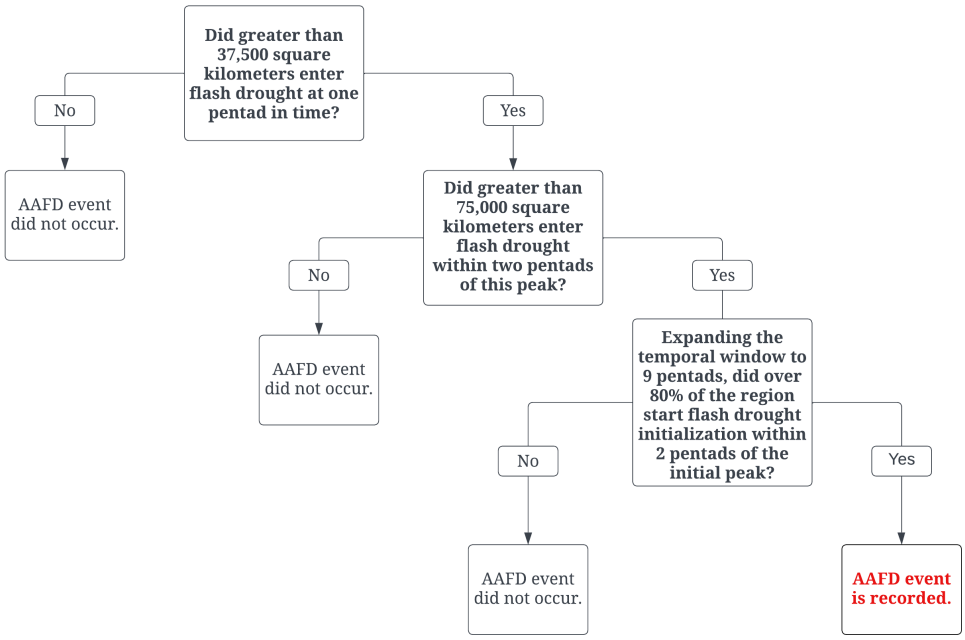

Figure 2.9: Flowchart diagram illustrating AAFD event criteria.

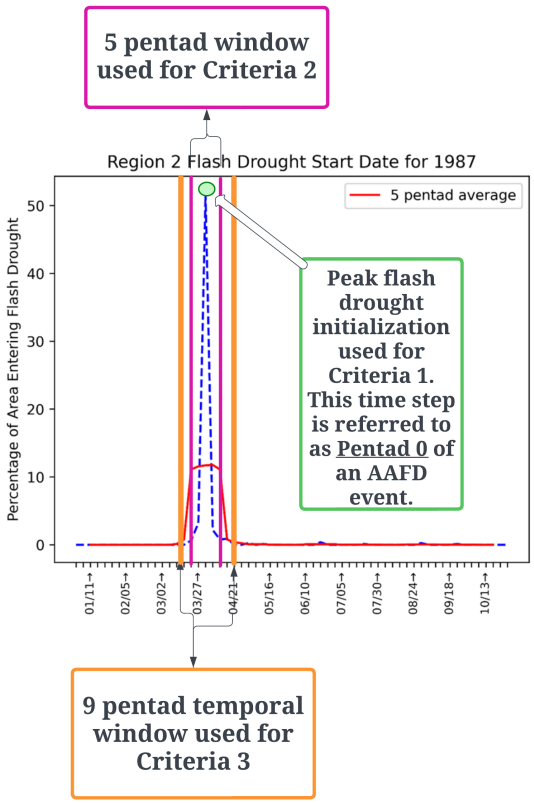

Figure 2.10: Physical representation of the Abrupt Agricultural Flash Drought methodology. It is annotated over a figure adapted from Figures 2.4a and 2.4b, but for an AAFD event recorded in the Midwest domain in 1987.

Chapter 3

Results

3.1 Spatiotemporal Occurrence of Flash Drought

The coverage of flash drought has varied significantly during the study period. Figure 3.1 displays the year-to-year spatial coverage of flash drought across both domains during the study period. Within Figure 3.1a, across the Southern Great Plains, flash drought coverage varied from less than 10 percent during some years (e.g., 1993 and 1996) to over 80 percent (e.g., 2000). Years with suppressed flash drought coverage, including 1993 and 1996, were pluvial years with above-average rainfall across the domain region that even produced significant flooding across the Midwest and Plains in 1993 (Bell and Janowiak 1995). This surplus in precipitation limited evaporative demand and flash drought experienced during these years. Conversely, years such as 2000 and 2012 yielded increased spatial coverage due to the more significant flash drought events that evolved during those years (Basara et al. 2013; Peters et al. 2002). Within the Midwest region, a similar trend in spatial coverage was observed. The pluvial year of 1993 resulted in suppressed flash drought coverage across the Midwest, with less than 10% of the area reaching flash drought criteria during the year (Figure 3.1b). However, in 1988, 2008, and 2012, rapid drought development occurred across at least three-quarters of the Midwest region.

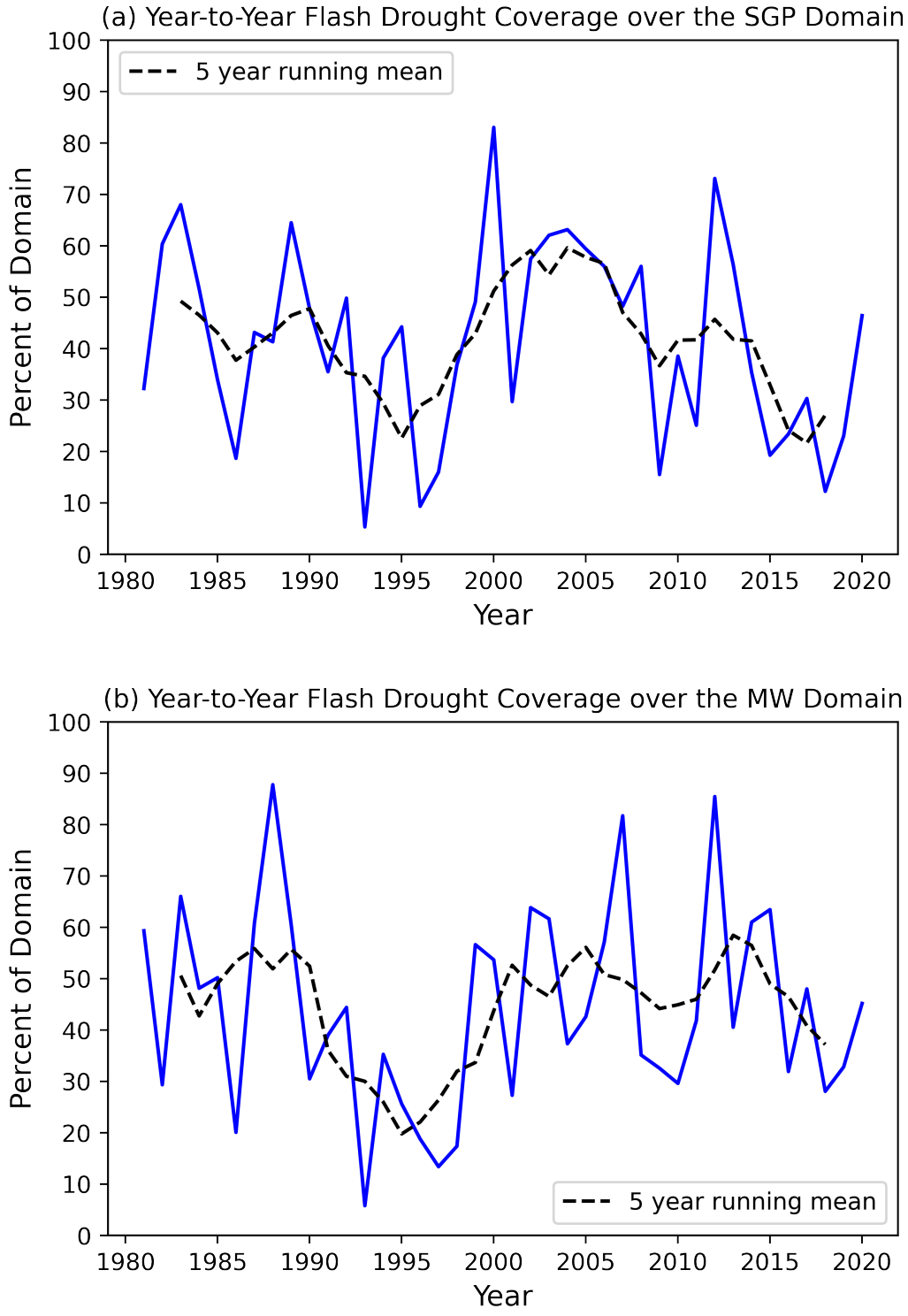

Figure 3.1: (a) Time series analysis of flash drought coverage from 1981 to 2020 (blue line) across the Southern Great Plains domain. The black dashed line represents a 5-year running mean. (b) Same as (a), but for the Midwest region.

Furthermore, temporal analysis reveals that the occurrence of when flash drought occurs has changed with time in both the Southern Great Plains and Midwest. In the Southern Great Plains, results initially show a peak in flash drought occurrence between April to June (Figure 3.2), with reduced activity present throughout the summer. A slight increase in flash drought occurrence is recorded during the fall months of September and October. These results follow consistently with flash drought activity in the western portions of the United States, as these regions typically experience a slight increase in flash drought occurrence in the fall (Christian et al. 2019a). When the study period is divided into two 20-year intervals, the temporal variability of the flash drought events yields differences in the timing of onset and occurrence. The first 20-year period spanning 1981 to 2000, illustrates that the late spring and summer months of May, June, and July had the highest occurrence of flash drought, with a secondary peak seen in the transition month of September (Fig. 3.2). Conversely, the second 20-year period from 2001 to 2020 displays two prominent periods of flash drought development during the months of April and October (Fig. 3.2). A pronounced increase in activity was also recorded in February, as over 10 percent of flash drought occurrences within this region between 2001 to 2020 started during this month.

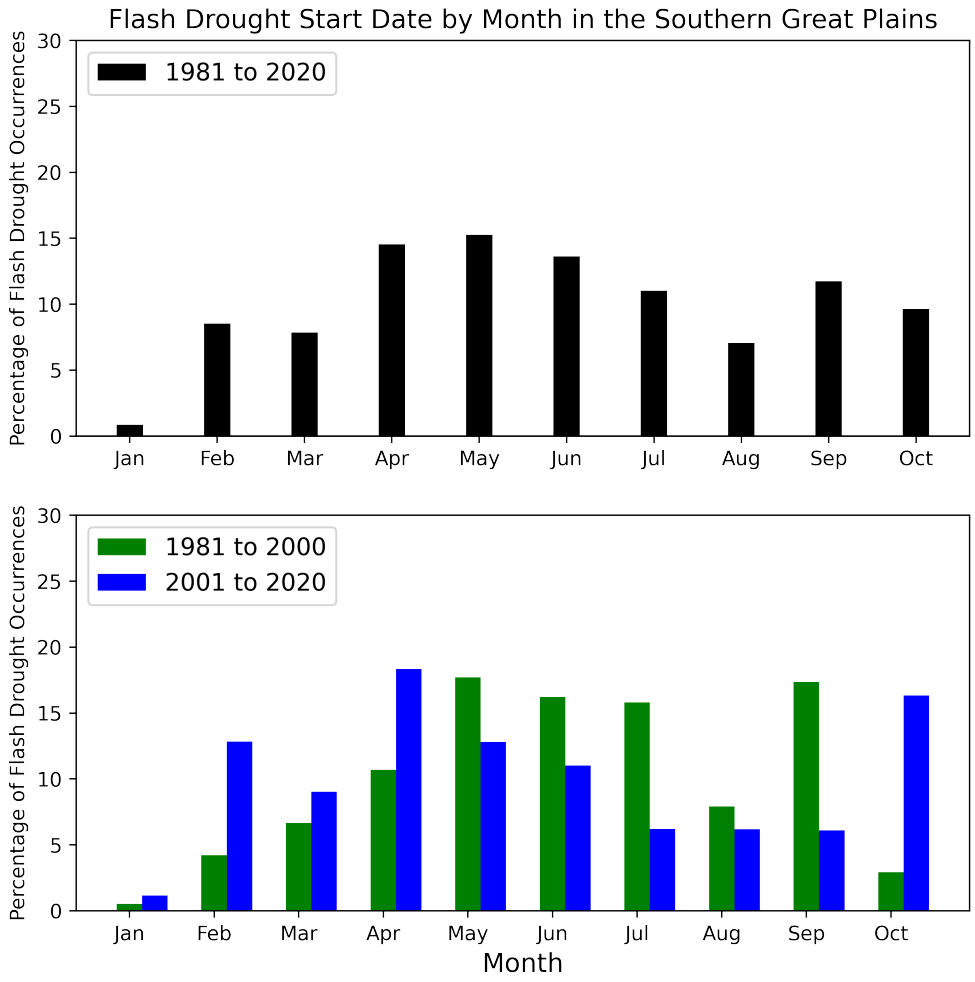

Figure 3.2: Temporal occurrence of flash drought across the Southern Great Plains domain from 1981 to 2020 (top panel) and from 1981 to 2000 versus 2001 to 2020 (bottom panel).

Within the Midwest agricultural region, the peak flash drought coverage occurred in the Spring months of April and May (Figure 3.3), slowly diminishing in occurrence during the summer and early fall months before a slight peak in October. From 1981 to 2000, more than 25% of all flash drought events began in April while the more recent 20-year period revealed flash drought occurring slightly later in the year, with

peak activity extending from May to July. From 2001 to 2020, approximately half of the flash drought events began during these three months.

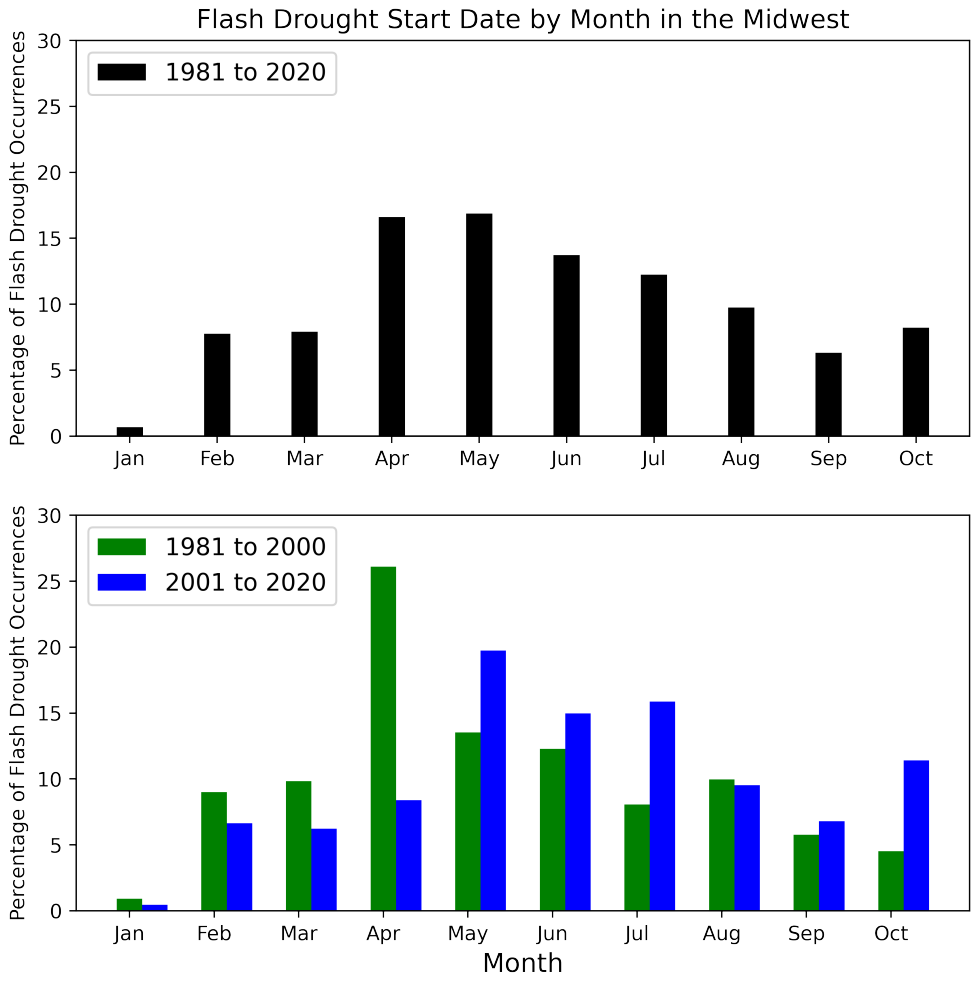

Figure 3.3: Same as Figure 3.2, but for the Midwest domain.

Lastly, the spatial climatology of flash drought occurrence was assessed. Figures 3.4 and 3.5 display the spatial variability of flash droughts over the SGP and Midwest regions, respectively, via the percentage of years whereby flash drought events were observed. Overall, the average grid point in the SGP region experienced a flash

drought in 40% of the years examined. While some areas within the domain experienced a flash drought in nearly three-quarters of the years, others experienced a flash drought in less than 30% of the period (Figure 3.4). The southwestern quadrant experienced fewer years with a flash drought while subregions in the north-central and eastern portions of the domain had increased occurrence. Past studies have demonstrated that over different regions of the world, flash drought occurrence can significantly vary across a small domain (Christian et al. 2019a; Edris et al. 2022; Lisonbee et al. 2022). These results further illustrate that flash drought behavior is highly heterogeneous, even across a mesoscale domain.

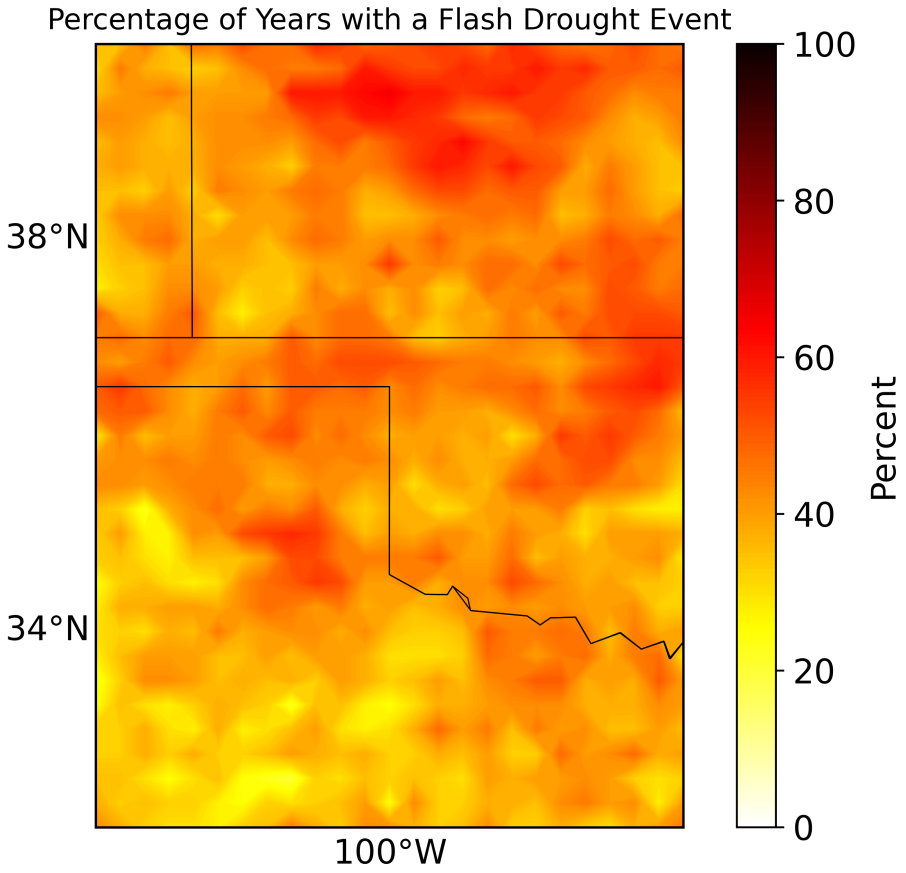

Figure 3.4: Percentage of years across the Southern Great Plains a flash drought event initiated during the defined growing season of March to October from 1981 to 2020.

Similar to the Southern Great Plains, the Midwest also experiences a large variability of flash drought events spatially (Figure 3.5). In the Midwest, there is a slightly higher average for the percentage of years a grid point experiences flash drought across the domain (45%). Many Midwest locations experienced flash droughts in over half of the years, while some areas experienced a flash drought in less than a third (Figure 3.5). The regions with the highest flash drought occurrences are generally seen in the southern portions of the domain, with less flash drought occurrence across the northern section of the region.

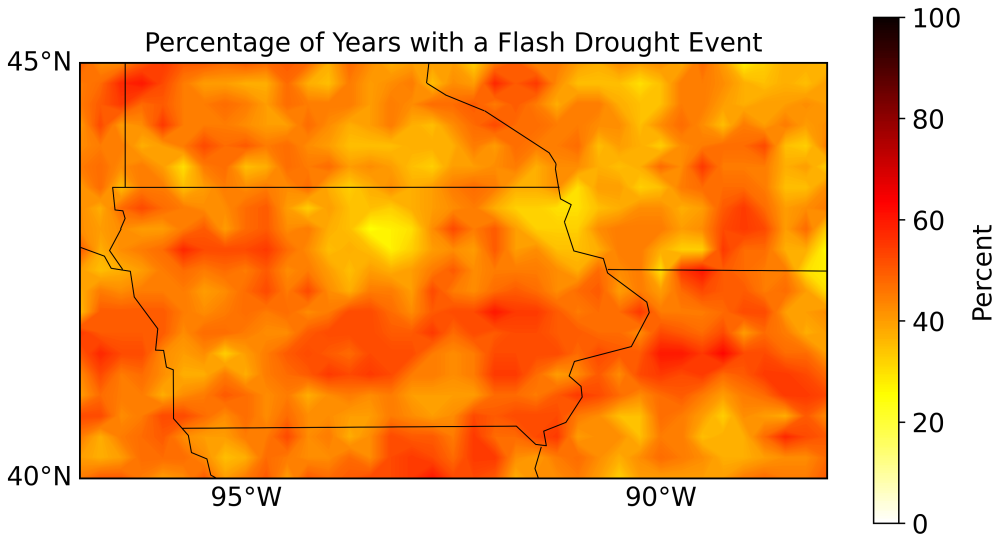

Figure 3.5: Same as Figure 3.4, but for the Midwest domain.

3.2 Abrupt Agricultural Flash Drought Analysis

3.2.1 Southern Great Plains

3.2.1.1 Spatial and Temporal Characteristics

Over the 40-year period, 32 AAFD events occurred within the Southern Great Plains region. Each event recorded across the Southern Great Plains can be examined in

Table A.1, depicting several key event characteristics, including timing, intensity, and spatial coverage. Initial analysis began by spatially plotting each of the events across the Southern Great Plains domain and dividing them into two 20-year periods (Figure 3.6). These results reveal that the occurrence and aerial coverage of these events has increased over time. Moreover, shifts have occurred in relation to AAFD hotspots. For example, across much of western and central Oklahoma, only 1 to 4 AAFD events were recorded from 1981 to 2000; however, results show 6 to 8 AAFDs occurred over much of this region from 2001 to 2020. Some of the highest concentrations of these events are collocated over extremely agriculturally dense portions of winter wheat, particularly in the eastern half of the domain south of Kansas (Lollato et al. 2017). Given plants and crops increase the moisture return out of the ground (Pereira et al. 1999) in response to increased evaporative demand, agricultural systems are particularly susceptible to these rapid drought events. Increases in the frequency of these events pose a high risk to stakeholders, as abrupt drought initiation results in decreased windows of time for agricultural producers to mitigate against these widespread events.

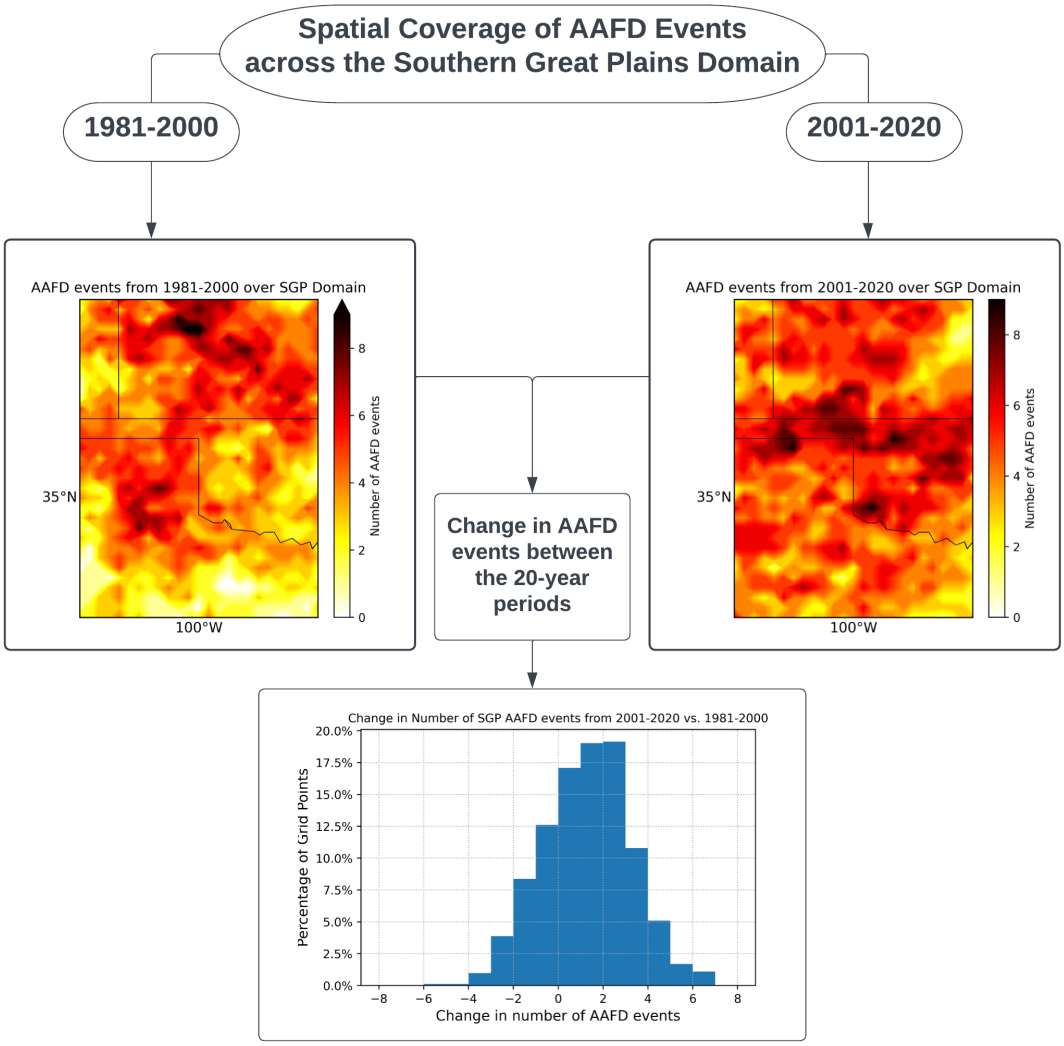

Figure 3.6: Spatial maps of AAFD events across the Southern Great Plains. This includes a spatial map of the number of AAFD events from 1981 to 2000 (top left), spatial map of the number of AAFD events from 2001 to 2020 (top right), and a histogram distribution of the changes in frequency of AAFD events at each grid point between the two 20-year periods.

Following spatial analysis of AAFDs over the SGP region, other event characteristics, including timing, event intensity, and aerial coverage, were analyzed, and are illustrated in Figure 3.7. AAFD events occurred consistently throughout the 40-year period. The 1990s featured several pluvial years, including 1993, which resulted in only 6 AAFD events during the second decade of the study. This prolonged period of above-average precipitation is highlighted in Figure A.2, depicting the average yearly

precipitation across Oklahoma to highlight this anomalous period of above-average precipitation. This surplus of precipitation reduced evaporative demand within the environment, thus inhibiting major flash drought development. Nonetheless, it highlights that in active pluvial periods, abrupt flash drought activity can remain a threat to this region. When analyzing the timing of events by month, AAFD initiation was observed every month of the growing season except for August. Further, results show that 11 of the 32 events started in September or October, indicating that fall AAFD events are prominent across this domain. These events, which occurred during the last two months of the study's defined growing season, were recorded in each decade, further conveying that fall abrupt flash droughts have consistently occurred during this study window.

Following the timing of AAFD events, the rate of change into drought was investigated to determine AAFD event intensity. To define event intensity for this study, the domain which entered flash drought within two pentads of the peak initialization (Pentad 0) was examined for each event, equating to a five-pentad temporal window. This timeframe was selected as a simple way to examine event progression for more than 80 percent of the AAFD event area, as this threshold must be met in Criterion 2 for AAFD identification. Next, the overall change in the standardized evaporative stress ratio (SESR) for the following six pentads was recorded over this defined region, equating to 30 days of investigation. This temporal window was selected to keep continuity with the flash drought duration outlined within Criteria 3 of the flash drought identification via SESR. For each grid point within this 5-pentad temporal window, the departure of SESR is averaged across the region. Following this, values were averaged temporally and expressed as an average rate of change in SESR per pentad in time.

Across the Southern Great Plains region, the intensities of AAFD events are decreasing with time. Changes to intensity may be linked to the overall aridification of the ground in the Southern Great Plains. It has been shown that the 100th meridian,

used to define the drier west from the moister east (Salley et al. 2016), may no longer mark this boundary. Studies including (Flanagan et al. 2017) have shown drought conditions can affect the location of this boundary and cause it to progress further eastward. Moreover, further studies have illustrated that soil moisture anomalies have and are likely to decrease in time across the Southern Great Plains (Dai 2013). As a result, it is likely that conditions within this domain have and will continue to become more arid in time (Seager et al. 2018). Semi-arid regions require relatively less evaporative demand to enter drought, thus reducing event intensity as the ground can only deteriorate to a certain extent. This logic also provides insight into overall flash drought occurrence. The southwestern portions of this domain experienced flash drought in only 25 to 40 percent of the years. The aridification of the ground over these regions is ongoing, causing these regions to be in semi-permanent drought-like states. One of the criteria for flash drought events is that a region must rapidly enter into drought. Any area in drought cannot experience a flash drought. As a result, these regions which remain in drought-like states will experience fewer flash drought events.

A final characteristic investigated for AAFD events was the spatial coverages of flash drought within each abrupt event. For each AAFD defined, at least 37,500 square kilometers of land entered flash drought criteria at one pentad. Moreover, several recorded events encompassing a significantly larger area entered rapid drought transition simultaneously. Between 2003 and 2012, five events (2003, 2004, 2006, 2008, 2012) recorded over 140,000 square kilometers of land beginning rapid drought intensification at one pentad in time. Four of these events began in the Spring and Summer months, while the event recorded in 2012 began at the end of October into the late Fall months of November and early December. When analyzing the average spatial coverage of Pentad 0 for each month of the year, May and July saw the greatest spatial regions entering flash drought at one pentad in time. Conversely, the spatial

thresholds are lower during later months such as September and October. During many of these AAFD events which occurred later in the growing season, some regions may be neglected from the event area as it is not the first flash drought occurrence a grid point within the domain has undergone during a specific year. Nonetheless, these results demonstrate that within the last 20 years, numerous flash drought events have simultaneously initiated across hundreds of thousands of square kilometers of winter wheat croplands.

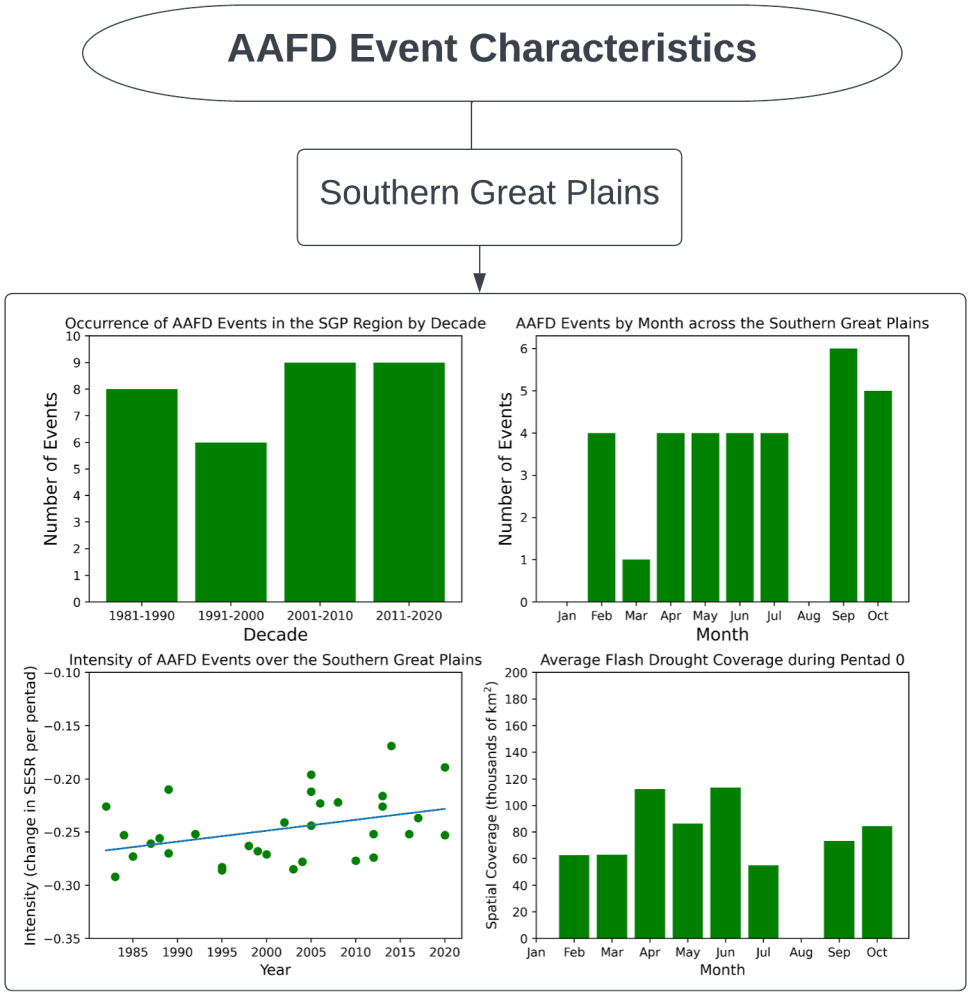

Figure 3.7: Properties of AAFD events across the Southern Great Plains domain. Plots within this diagram include the number of events per decade from 1981-2020 (top left); the number of events by month (top right); the intensity of AAFD events in time, expressed in units of change in SESR per pentad (bottom left); and the total aerial coverage of AAFD events at Pentad 0 for each month of the year (bottom right).

3.2.1.2 AAFD timing in relation to ENSO

Across the Southern Great Plains, teleconnections can be essential in preconditioning the synoptic environment to impact crop health and yields (Mauget and Upchurch 1999). Given that crops are susceptible to changes in temperature and precipitation, different teleconnection regimes can pose dramatically different impacts on crops.

One of the significant teleconnections which cause fluctuations in precipitation and temperature across the United States is the El Niño Southern Oscillation (ENSO). ENSO, dictated by temperature anomalies recorded over regions of the Pacific Ocean, includes two main phases: El Niño and La Niña (NOAA, NCEI 2009). Using the Oceanic Nino Index (ONI), anomalies of the sea surface temperatures (SSTs) provide information regarding the ENSO phase and strength, which is then expressed as an anomaly number. When ONI becomes less than or equal to -0.5, it is stated that the atmosphere is in a La Niña regime. When ONI is greater than or equal to 0.5, this phase of ENSO is referred to as El Niño. ONI values that fall between these thresholds are considered to be in the neutral stage of this teleconnection. Across the Southern Great Plains, La Niña periods typically result in decreased precipitation due to a northward shift of the Jetstream due to amplified ridging off the West Coast (Trenberth and Branstator 1992; Shabbar and Yu 2009). Moreover, it is known that certain phases of this teleconnection can generally affect winter wheat crop yields. Across the southeastern United States, La Niña regimes on average lead to higher winter wheat yields (Woli et al. 2015) whereas winter La Niña regimes from November to January lead to statistically significant lower yields across the central United States (Mauget and Upchurch 1999). Thus, it was of interest to investigate if abrupt flash drought events occur more commonly in specific regimes of ENSO, and the effect these regimes may have on crop yields.

Figure 3.8 indicates the ENSO signal through ONI during the 32 AAFD events recorded across the Southern Great Plains. Figure 3.9 then illustrates each ONI value into bins to view as a histogram. Overall, there is a slight increase in AAFD events occurring with negative ONI values, specifically those between 0 to -0.5. Nine events occurred during a La Niña phase as opposed to only four AAFDs during the El Niño regimes. Furthermore, no abrupt flash drought events have occurred in conjunction with an El Niño phase within the last 20 years. Previous studies, including Chen et al. (2019), suggested that La Niña regimes increase flash drought across the central

United States. Sustained periods of La Niña conditions were recorded from 1998-2001, 2010-2012, and, most recently, from 2020-2022. Major flash droughts were recorded during these extended periods of the La Niña regime (Peters et al. 2002; Basara et al. 2013, 2019). These results are also seen within the AAFD database across the Southern Great Plains, as multiple abrupt flash droughts were recorded over the first 2 extended periods (Table A.1). Given that the winter La Niña regime typically results in decreased precipitation across the Southern Great Plains, investigation of this ENSO phase concerning abrupt flash drought timing and subsequent impacts followed.

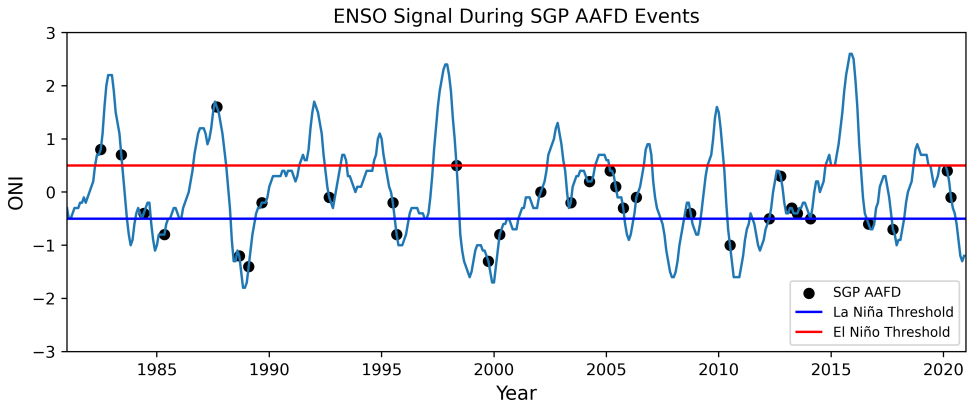

Figure 3.8: 3-month averaged ONI from 1981 to 2020. The blue (red) line marks the threshold needed for ONI to be considered a La Niña (El Niño) phase. Black stipples represent SGP AAFD events and is plotted for the month that Pentad 0 was recorded for each abrupt flash drought.

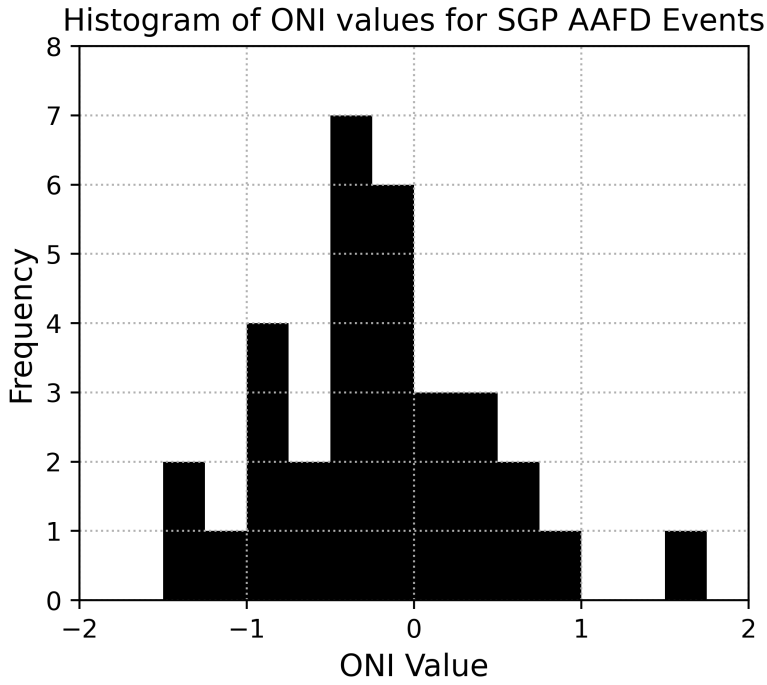

Figure 3.9: Histogram distribution of the three-month averaged ONI value during peak initialization for an AAFD event within the Southern Great Plains domain.

3.2.2 Midwest

3.2.2.1 Spatial and Temporal Characteristics

Analysis was also performed for the United States Midwest region for AAFD events. Across this region, 23 events were captured during the 40 years (Table A.2). While only nine events occurred from 1981 to 2000, 14 were recorded from 2001 to 2020 with eight in the most recent 10-year period. Spatial analysis of these events provides essential insight into the potential changes in location and occurrence of abrupt flash droughts being documented within this region of the country.

Figure 3.10 illustrates the spatial coverage of Midwest AAFD events across the two 20-year study periods of 1981-2000 and 2001-2020. From 1981 to 2000, the highest occurrence of these events was recorded across the southeast portion of the domain, with far eastern Iowa and northern Illinois recording the greatest frequency of

events. During the following 20-year period, the frequency and hotspot of abrupt flash droughts changed. The most significant increases in abrupt flash drought occurrence were observed across central portions of the domain, extending from southern Missouri into southern Wisconsin, encompassing most of Iowa. Increases in AAFD coverage are illustrated in Figure 3.10 as well, as the histogram conveys an overall increase in AAFD events across a large majority of the region. In some locations, the number of AAFD events experienced between 2001 to 2020 increased by three to seven compared to the earlier period.

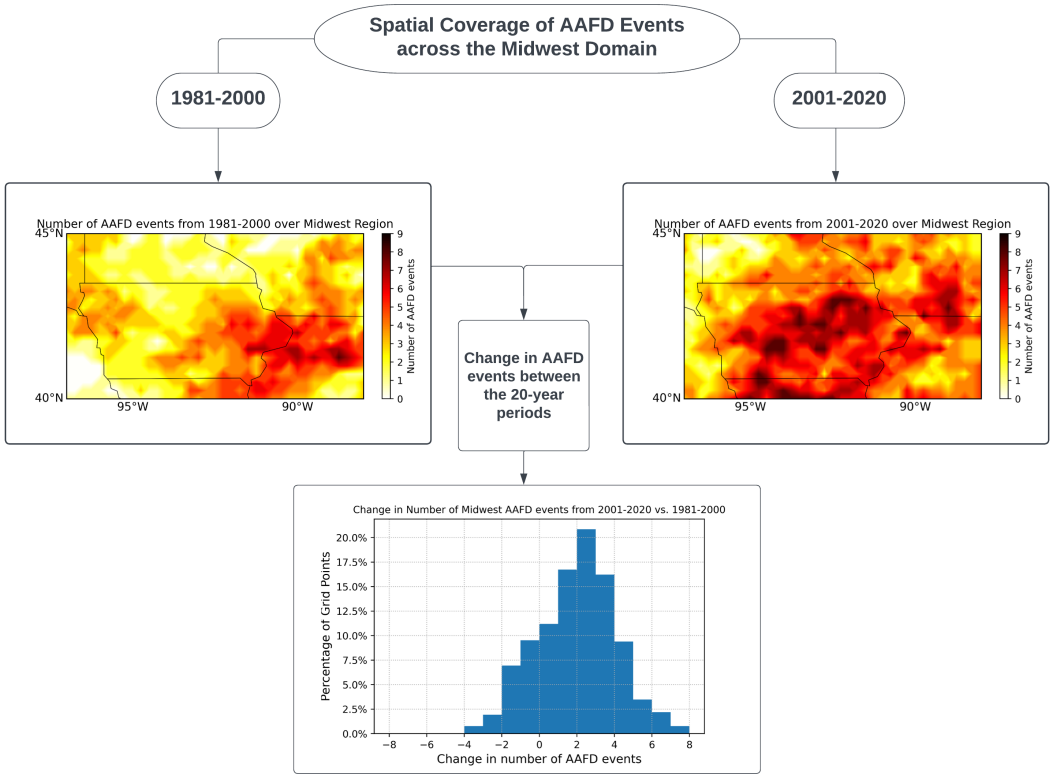

Figure 3.10: Same as Figure 3.6, but for the Midwest region.

AAFD characteristics were also examined for the Midwest region, as seen in Figure 3.11. Assessment of AAFD events by decade reveals AAFD events occurred in every decade across the Midwest domain, with a decrease in event occurrence during the pluvial period over the 1990's. The timing of AAFD events across the Midwest region varies considerably from the Southern Great Plains region. Across the Midwest,

AAFD events initialized in every month of the growing season aside from September. A clear peak in events exists during the late Spring and early summer months. More than a quarter of all AAFD events started in May, and over half (13 of 23 AAFD events) were initiated during April, May, and June. This highlights that abrupt flash drought behavior in the Midwest is most prominent during the late spring and early summer months. On the contrary, only two AAFD events were recorded across the Midwest during the fall months of September and October. This result differs significantly from Southern Great Plains, as over a third of the AAFD events recorded in the SGP domain started in September and October. These temporal results demonstrate that abrupt flash drought behavior and timing are highly variable even amongst these two spatially close regions.

Within the Midwest a slight increase in AAFD intensity over time was observed. During the nine events recorded from 1981 to 2000, the most "intense" abrupt flash drought occurred in 1987 with an average departure of SESR of -0.263 standard deviations per pentad. Between 2001 and 2020, out of the 14 events observed, six had a more vigorous intensity than the AAFD in 1987. Moreover, four of these six events were recorded between 2014 and 2017. AAFD intensity for each event in the Midwest is displayed within Figure 3.11, confirming that event intensity in time differs from what was seen in the Southern Great Plains. While there may not be a significant trend of increasing event strength, evidence demonstrates that AAFDs in the most recent decade have recorded a larger departure in SESR values during the rapid intensification process. Furthermore, it conveys that flash drought occurrence, timing, and intensification have changed in time uniquely across the Midwest and Southern Great Plains domains.

Lastly, the spatial extent of each event was examined across the Midwest region. Over this domain, there was high variability in the spatial coverage of events recorded at Pentad 0. The most outstanding spatial coverages during abrupt flash droughts occurred in July; however, significant flash drought coverage also occurred for events

that began during February and April. In each of these months, over 100,000 square kilometers began a rapid drought transition within one pentad.

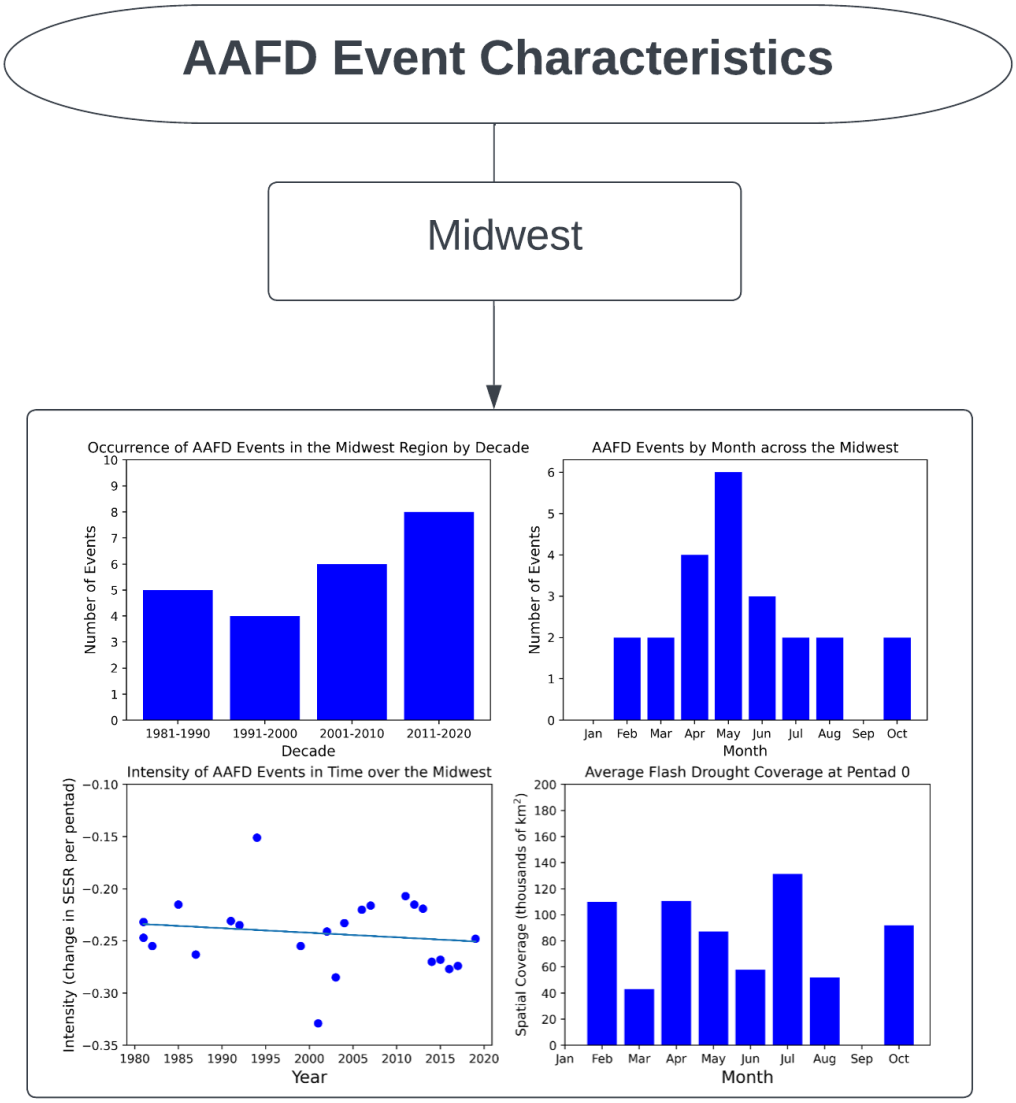

Figure 3.11: Same as Figure 3.7, but for the Midwest region.

3.2.2.2 AAFD timing in relation to ENSO

The timing of AAFD events in the Midwest in conjunction with ENSO was also investigated within this study, Figure 3.12 depicts AAFD events in the Midwest in relation to ONI. Figure 3.13 further illustrates these ONI values in a histogram

distribution. In comparison to the Southern Great Plains domain, more events did occur in the Midwest domain during an El Niño regime. The Midwest had 8 AAFD events occurring during an El Niño pattern, double the number of cases experienced during the same regime across the Southern Great Plains. Several Midwest events (1982, 1987, 1991, and 1992) were initiated during an El Niño regime from April to June. Figure A.3 illustrates the precipitation anomalies and trends across the United States during the El Niño phase for these three months. There are vast differences in precipitation anomalies between the Southern Great Plains and the Midwest during these El Niño regimes in the late spring/early summer timeframe. Across the Southern Great Plains domain, El Niño regimes during this time typically lead to above-average rainfall periods. In contrast, negative precipitation anomalies are seen across most of the Midwest. Prolonged periods of precipitation deficits during these regimes can aid in the development of flash drought across the Midwest while supporting suppressed flash drought activity across the Southern Great Plains with climatologically increased periods of precipitation.

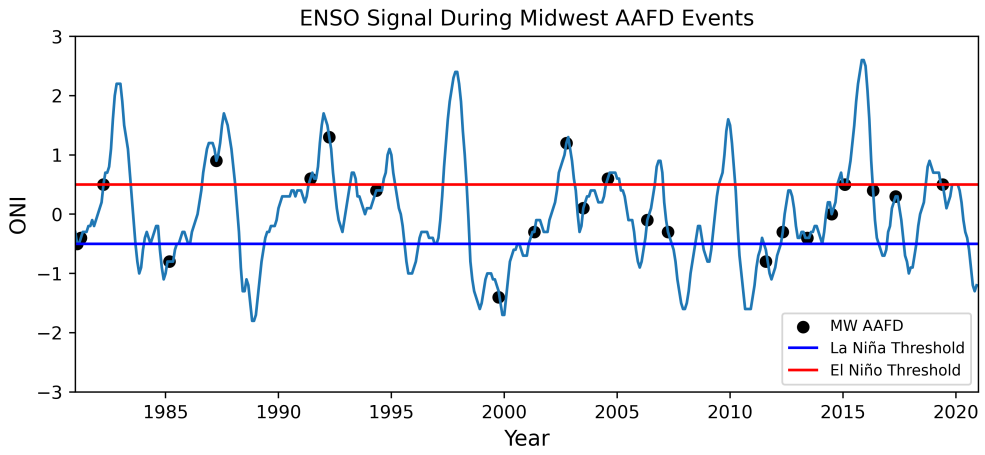

Figure 3.12: Same as Figure 3.8, but for the Midwest region.

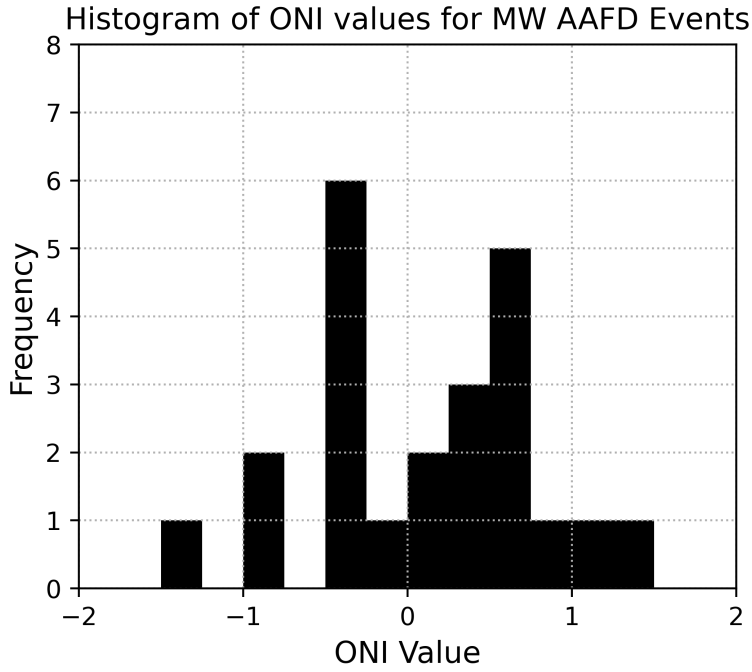

Figure 3.13: Same as Figure 3.9, but for the Midwest region.

Chapter 4

Discussion

4.1 Southern Great Plains

Every year, tens of millions of acres of winter wheat are harvested across the Southern Great Plains. Kansas has repeatedly yielded the greatest winter wheat harvest in this region. In 2022, 364 million bushels of winter wheat were harvested in Kansas, and almost 200 million bushels were collected in Oklahoma and Texas cumulatively (USDA, NASS 2022). Figure 4.1 illustrates the timing of each growing stage of winter wheat from 2015 to 2020 for the state of Oklahoma, following closely to the growing seasons of winter wheat in Texas and Kansas. During September to October, winter wheat is planted across the region with emergence a few weeks later followed by dormancy during the winter. As surface temperature warms during the months of March and April, winter wheat matures with crop harvest during the late spring months into early summer. The exact timing of the harvest depends on the atmospheric conditions throughout the spring time frame and by latitude, as crops further south within the domain typically have an earlier harvest than those farther North (Sacks et al. 2010).

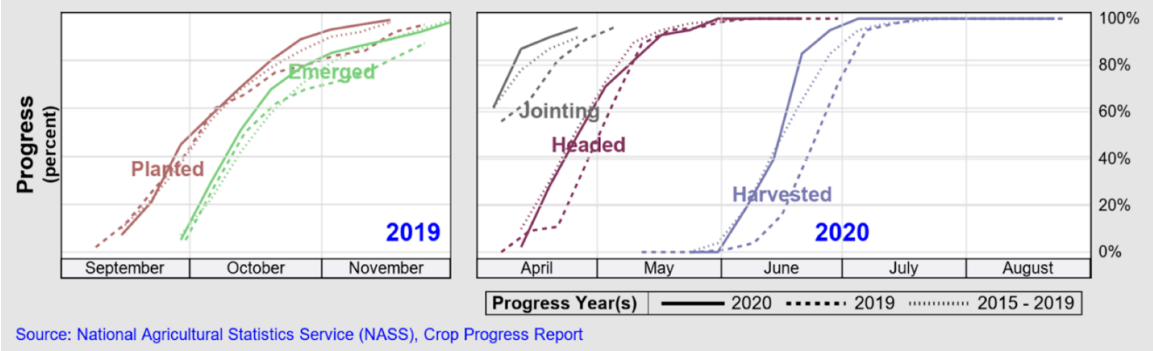

Figure 4.1: Crop growing season calendar for winter wheat in Oklahoma, including the planting stage (brown lines), emergence (green lines), jointing (gray lines), heading (maroon lines) and harvest (periwinkle lines). The solid line (dashed line) represents the timing of winter wheat during the 2019-2020 (2018-2019) growing season. The thinly dashed line represents a five-year average from 2015-2019. (USDA, NASS)

From an agricultural perspective, it is well-known that soil moisture is critical for the health of winter wheat (Kansas State College of Agriculture and Applied Science 1936). Moreover, this fact becomes extremely important when assessing winter wheat behavior across this domain. Within the Southern Great Plains, the soil moisture has a periodic, seasonal cycle that occurs each year. Illston et al. (2004) studied these changes across Oklahoma and found that soil moisture at several soil depths varies seasonally. Specifically, a rapid decline in the Fractional Water Index begins during the summer months of July into August and September. At the beginning of fall, a sharp increase in soil moisture occurs due to decreased ET and increased precipitation. As a result, flash drought events during this window of fall recharge may pose a severe risk to the suitability of soil during the winter wheat growing season. To address this question, analysis began to understand how these abrupt flash drought events coinciding with critical times during the moisture cycle of soil affect crop health and overall yields.

Data from the USDA analyzing crop conditions were used to investigate the impact of flash drought events on crops during different times of the growing season. Crop conditions are examined through weekly crop progression data from the USDA NASS

that is evaluated to track winter wheat during the Spring months. From 2001-2020, seven years occurred (2005, 2008, 2010, 2012, 2013, 2016, 2017) where abrupt flash drought events initiated between July and October (Table A.1). More specifically, 2005, 2008, 2012, and 2017 recorded an AAFD beginning in October, when winter wheat planting was underway.

Figure 4.2 displays the percentage of winter wheat crops in good and excellent health across Oklahoma from 2001 to 2020. During years with an AAFD between July and October, winter wheat sustained reductions in crop health the following growing season. In all but one of these years, the percentage of winter wheat crops in good and excellent health persistently remained less than 30 percent, up to the time of harvest. Further, the six worst crop condition reports occurred when an abrupt flash drought was recorded in the prior year from July to October. Moreover, during all other years from 2001 to 2020, the percentage of crops listed as "excellent" or "good" was, on average, much higher, even during years that recorded abrupt flash drought events within the primary growing season in the Spring. One example is 2012, as this flash drought impacted most of the central United States and was recorded as an AAFD event in the SGP domain beginning in early April (Table A.1). At the end of the 2012 winter wheat growing season, reports showed that the overall yield significantly recovered compared to the yields seen in all three states during the prior growing season in 2011 (USDA, Economic Research Service 2015). Focusing on 2011, while no abrupt flash droughts were recorded during the growing season, an abrupt flash drought was recorded during the previous summer between growing seasons (initiated mid-July 2010). Drought conditions persisted through the fall and winter months into the spring across the Southern Great Plains (Figure A.4), resulting in decreased yields in all 3 states from the year before. These results demonstrate that abrupt flash drought events from July to October may severely impact winter wheat health and yields during the following growing season. As a result, future efforts focused on understanding if AAFD events from July to October consistently impact

winter wheat conditions the following year within Oklahoma and the Southern Great Plains overall. Furthermore, it led to the investigation as well of understanding what winter patterns could drive unhealthy growing conditions for winter wheat crops, such as soil moisture, during the following spring.

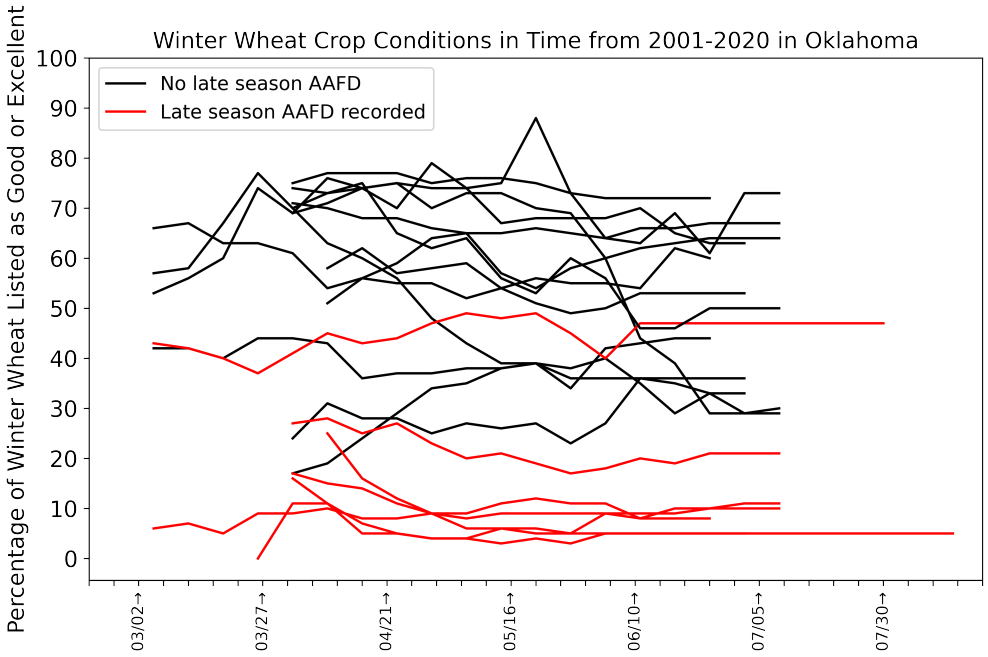

Figure 4.2: Time series analysis of weekly crop conditions during winter wheat growing seasons across Oklahoma from 2001-2020, highlighting the percentage of crops listed in good or excellent condition. Red lines indicate the crop conditions for winter wheat of years which followed an AAFD event recorded between July to October. All other growing seasons are included as black lines.

Nine of 15 AAFD events (1988, 1995, 1999, 2005, 2008, 2010, 2016, 2017) during the 40-year period which began between July to October also occurred in conjunction with a winter La Niña. All winter La Niña periods from 1981 to 2020 are illustrated in Table A.3. In some of these years, La Niña conditions were also present during the summer; however, during some part of these winters, a La Niña signal was present. During the winter months across the Southern Great Plains, precipitation is limited (Seager et al. 2018). In La Niña regimes, precipitation departures are more pronounced (Pu et al. 2016). Figure 4.3 illustrates this point even further, displaying

the temperature and precipitation distributions experienced December to February during each of the 3 ENSO regimes (El Niño, Neutral, La Niña) for several climate divisions located within the Southern Great Plains domain (Climate Prediction Center). Across much of the western and central portions of the domain, El Niño regimes typically result in larger amounts of precipitation across the domain. Moreover, during neutral and specifically La Niña periods within these regions, an overall decrease in precipitation occurs within the area along with increased temperatures. Although the overall amount of rain varies, these departures are significant for the time of the year they are occurring. This led the investigation of how La Niña regimes may impact winter wheat crop yields across each state in the SGP domain.

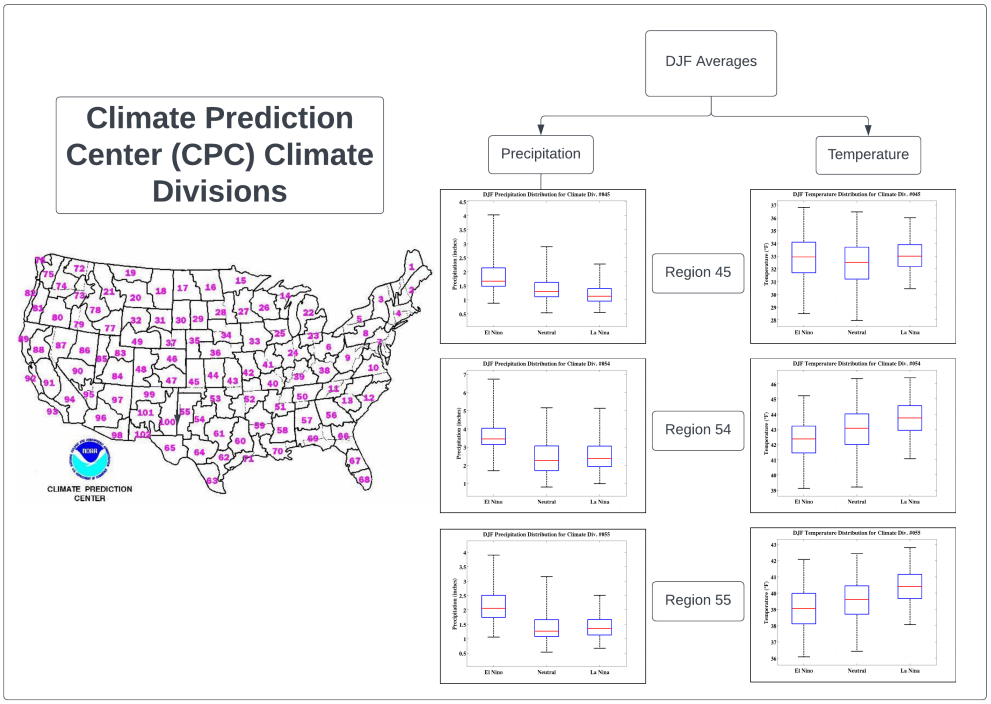

Figure 4.3: DJF averaged temperature and precipitation box and whisker plots for regions 45, 54, and 55 during El Niño, Neutral, and La Niña regimes. Each plot illustrates the distribution of temperature and precipitation during these months for each active regime from 1950 to present day (Climate Prediction Center 2023).

,

Figure 4.4 depicts the winter wheat yields across Kansas, Oklahoma, and Texas from 1981-2020. Black and red stipples represent the yields of winter wheat obtained during the growing seasons of years that followed a winter La Niña. Black stipples indicate winter wheat yields following an abrupt flash drought recorded from July to October of the prior year with a La Niña winter regime. Red stipples are indicative of years without an AAFD from July to October with a winter La Niña signal. The results indicate that for a majority of years where (1) an abrupt flash drought late in the calendar growing season followed by (2) a La Niña winter period, winter wheat yields were reduced during almost every year across all three SGP states. Moreover, crop yields were much closer to a standard yield during years without an abrupt flash drought in the last summer or fall and a winter La Niña regime.

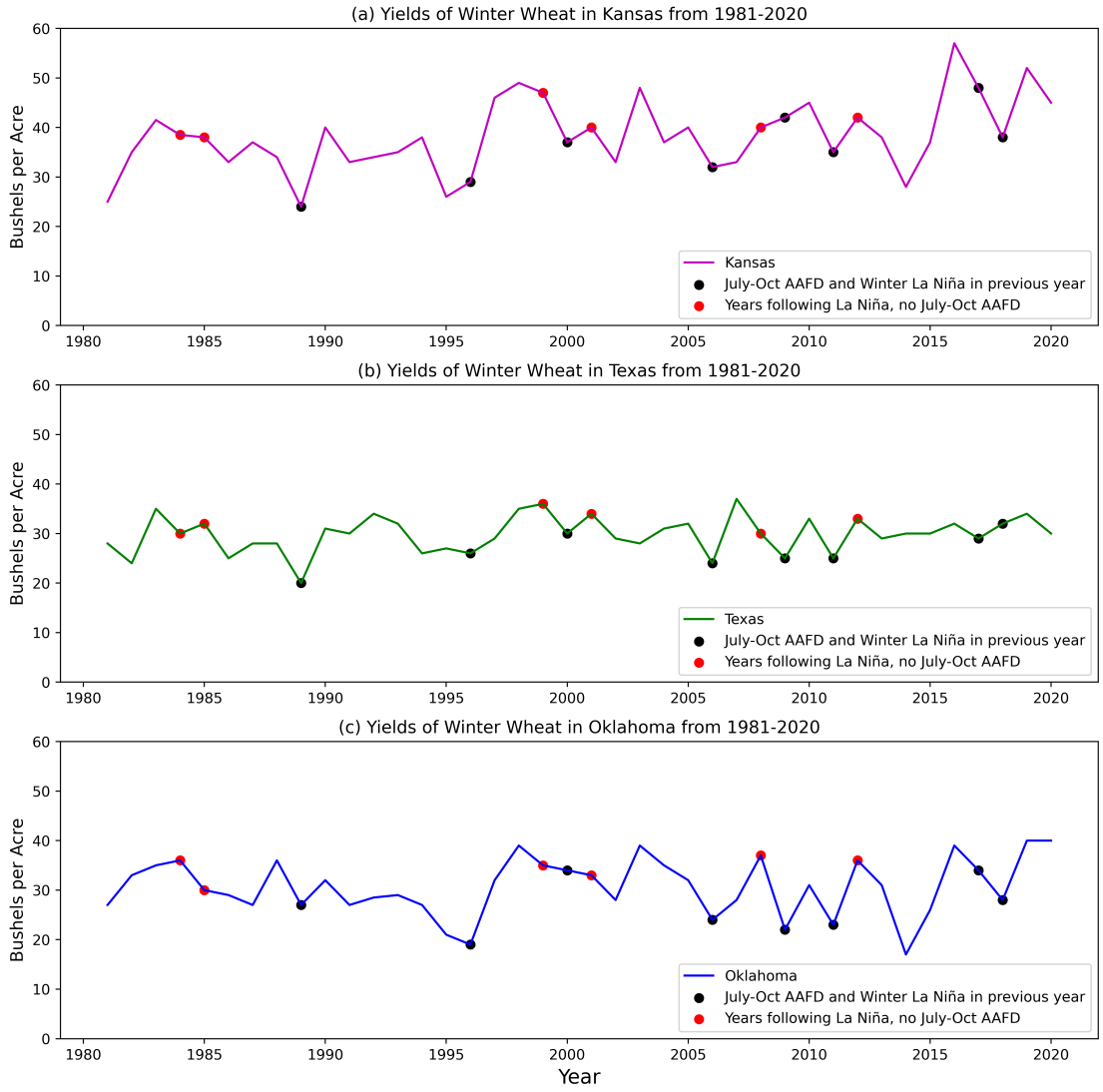

Figure 4.4: (a) Winter wheat yields from 1981 to 2020, reported from the USDA NASS for the state of Kansas. Yields are reported in units of bushels per acre. Black stipples represent the yields of years following a July to October AAFD event and a winter La Niña. Red stipples indicate crop yields of years following a winter La Niña pattern and no July-October AAFD event. (b) Same as (a), but for Texas. (c) Same as (a), but for Oklahoma.

To quantify how anomalous winter wheat crop yields are during specific groups of years, statistical testing was conducted using bootstrap testing. This statistical technique required obtaining 10,000 random samples of data from the crop yields reported across each state. This technique allows one to understand where crop yields respectively fall onto this distribution to illustrate the departures that may be noted

during specific years. Furthermore, given each dataset had a unique distribution, this statistical technique was applied, as bootstrapping can work on any statistical distribution. Prior to completing statistical testing, crop yields were linearly detrended as advancements in crop biodiversity have caused general increases in wheat productivity over time (University of Minnesota 2023). Results from the statistical testing illustrate the impacts AAFD events in conjunction with a winter La Niña pattern have on crop yield (Figures 4.5-4.7). To begin, focusing on Texas (Figure 4.5), statistical testing concludes on average, winter La Niña conditions result in decreased winter wheat yields overall during the 40-year period, concurring with previous studies (Mauget and Upchurch 1999). However, a breakdown of La Niña years into those that had an AAFD prior to the Winter between July to October versus years that did not yield critical results. During years without an AAFD during that time, winter wheat yields are anomalously high, with the average yield at or above the 80th percentile across Texas. On the contrary, during years with a July to October AAFD followed by a winter La Niña pattern, crop yields on average are anomalously low. Across Texas, winter wheat yields during these years were on average at or below the 20th percentile. Within Oklahoma (Figure 4.6), winter wheat yields during years with both a July-October AAFD and winter La Niña regime are also anomalously low, on average below the 20th percentile. During La Niña winters without an AAFD occurring prior, yields were on average above the average recorded over the 40-year period. Across Kansas (Figure 4.7), similar results arise. While crop yield departures are not as significant compared to Texas and Oklahoma winter wheat yields, it is still noted that AAFD events in conjunction with a winter La Niña pattern on average result in decreased winter wheat yields. Moreover, evidence also suggests that during years with a winter La Niña pattern and no AAFD event, winter wheat yields are typically above average.

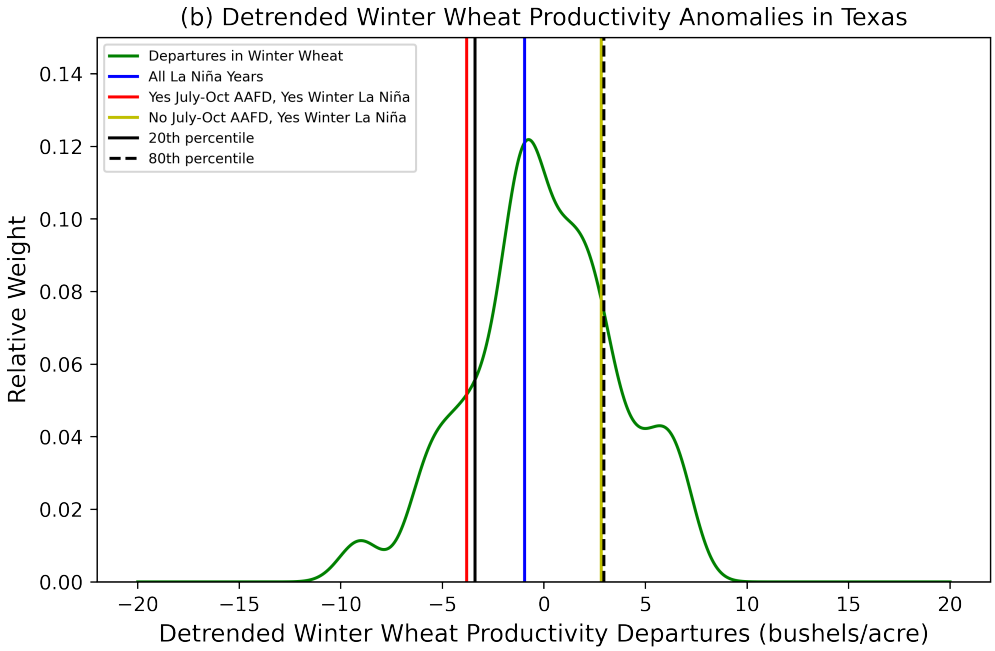

Figure 4.5: Bootstrapping (n = 10,000 iterations) statistical testing for winter wheat yields across Texas from 1981-2020. The plot contains the probability density function of winter wheat yields (green line), 20th percentile threshold (dark black line), 80th percentile threshold (black dashed line), average yield during all La Niña years (blue line), average winter wheat yield during years with an AAFD from July to October and winter La Niña (red line), and average winter wheat yields for years without an AAFD from July to October and a winter La Niña (yellow line).

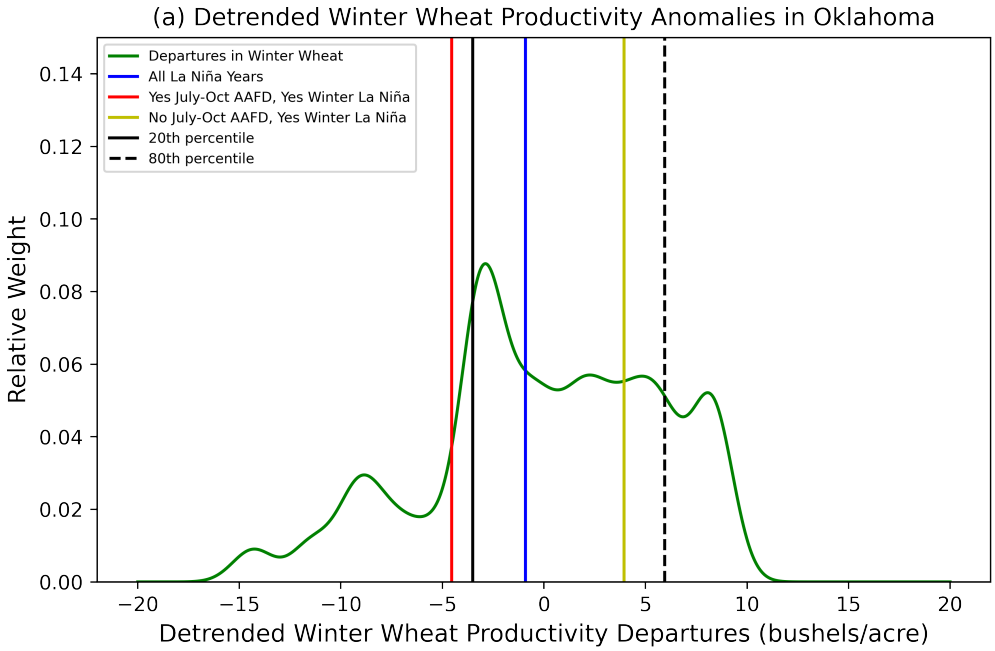

Figure 4.6: Same as Figure 4.5, but for Oklahoma.

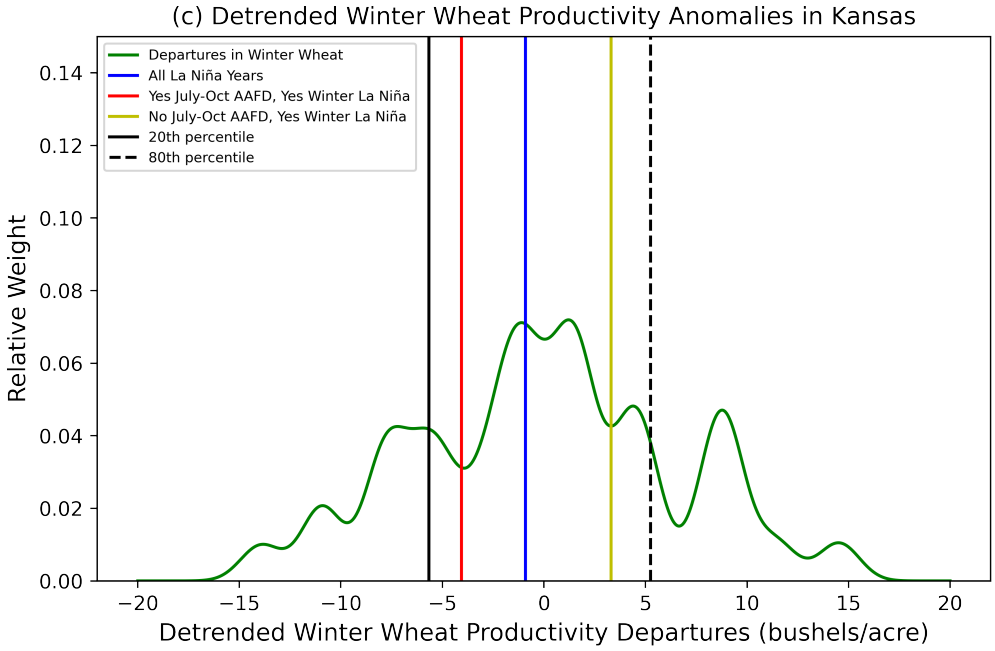

Figure 4.7: Same as Figure 4.5, but for Kansas.

These results indicate that a La Niña pattern can lead to decreased winter wheat yields the following year. However, these most significant departures are experienced during years when both a winter La Niña regime is in place and an abrupt flash drought period occurred during the previous summer or fall. Given that these areas experienced a flash drought during the summer or fall, ground conditions have significantly reduced soil moisture due to reduced precipitation. These prolonged precipitation and soil moisture deficits, stemming from these flash drought events, result in stressed crop conditions for the duration of the winter wheat growing season, causing significantly lower winter wheat yields.

The differences in soil moisture anomalies can be compared between the two groups of years to quantify these departures in soil moisture. Soil moisture composite anomalies are illustrated for each group of years at three timesteps: the beginning of July, the beginning of December, and the beginning of March. Figure 4.8 displays the composite anomalies for the eight years where an AAFD from July to October occurred in conjunction with a winter La Niña. Figure 4.9 illustrates the composite anomalies for the six years where an AAFD did not occur from July-October, but a winter La Niña was present. At each time interval, statistical testing via bootstrapping (n = 5,000 iterations) was also completed to determine if soil moisture anomalies were statistically significant for the group of years when compared to climatology. At the beginning of July, soil moisture anomalies for both groups of years remain close to climatology. However, during years with an abrupt flash drought recorded from July to October, statistically significant negative moisture anomalies were prevalent across most of the southern United States in early December. For the years when no flash drought occurred, there were positive soil moisture anomalies across much of the Southern Great Plains at this time. By the beginning of March, we see that for years with an abrupt flash drought followed by a winter La Niña pattern, soil moisture anomalies have returned to climatology across most of the Midwest and Southeast. However, these statistically significant negative soil moisture anomalies continue to

persist across portions of the Southern Great Plains. During years with just a winter La Niña regime, soil moisture anomalies remained above climatology for the start of the growing season.

Statistical testing was completed as well to determine the magnitude of difference in soil moisture anomalies present across this region at the start of the Spring growing season (beginning of March) via bootstrapping (n = 5,000 iterations with a significance level to the 95th percentile). These results displayed in Figure 4.10 confirm that a statistically significant difference in the soil moisture anomalies was present at the start of the growing season across a majority of the Southern Great Plains region when comparing these two groups of years. Moreover, we see there is a sharp cutoff in these soil moisture composite differences further east and north. These results further highlight that deficits in soil moisture beginning with an AAFD event persist throughout the winter and into the spring, likely negatively affecting winter wheat yields in the Southern Great Plains. Moreover, this analysis also demonstrates that La Niña patterns alone do not decrease winter wheat yields the following growing season. The combination of an abrupt flash drought followed by a winter La Niña pattern leads to extended periods of soil moisture desiccation, resulting in lower winter wheat yields on average across the SGP region.

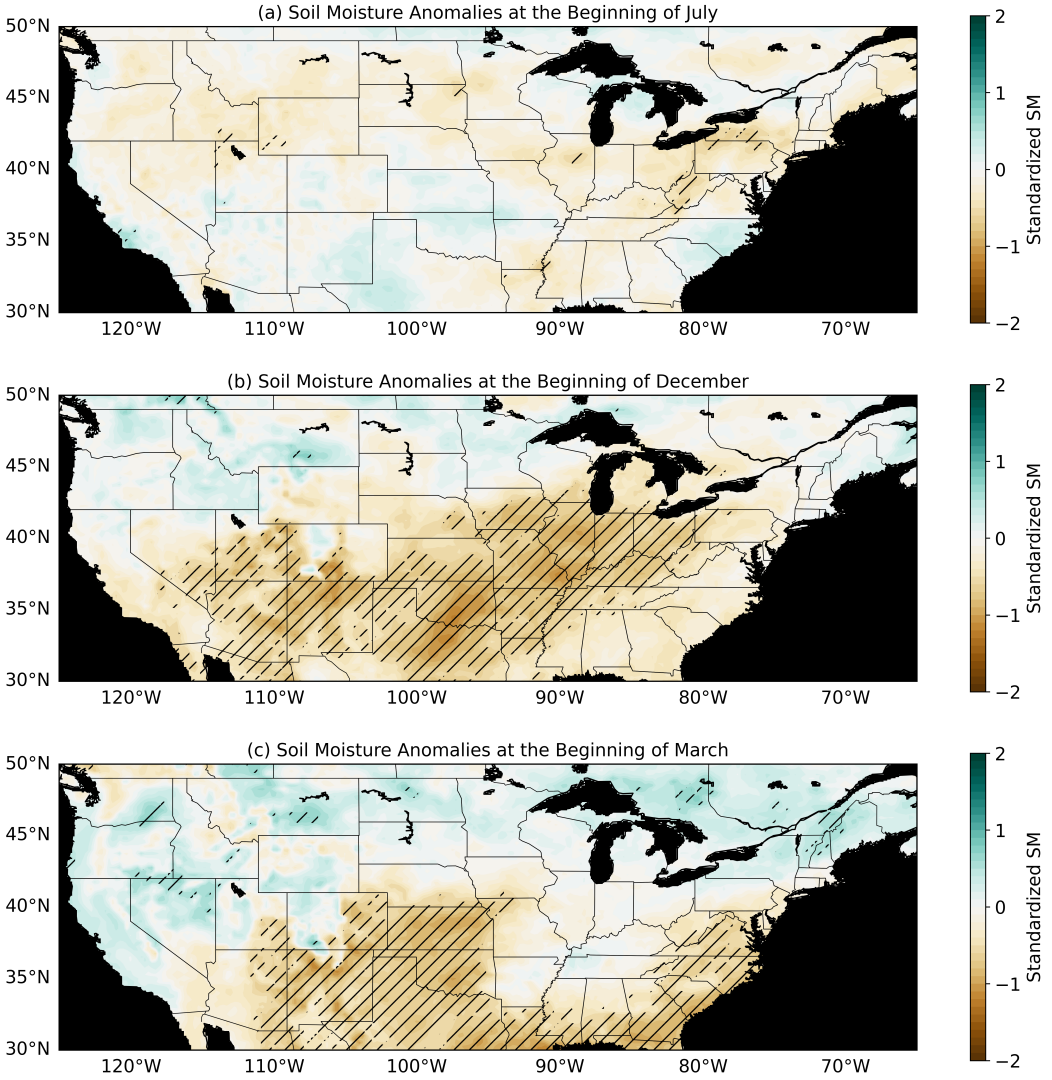

Figure 4.8: Composite standardized soil moisture anomalies for years when an AAFD occurred from July-October across the Southern Great Plains domain followed by a winter La Niña regime. The plots contain the averaged soil moisture anomalies for three pentads of time: The beginning of July (top figure), the beginning of December (middle figure), and the beginning of March (bottom figure). Hatching indicates statistically significant departures in soil moisture anomalies to the 95th percentile through bootstrapping (n = 5,000 iterations).

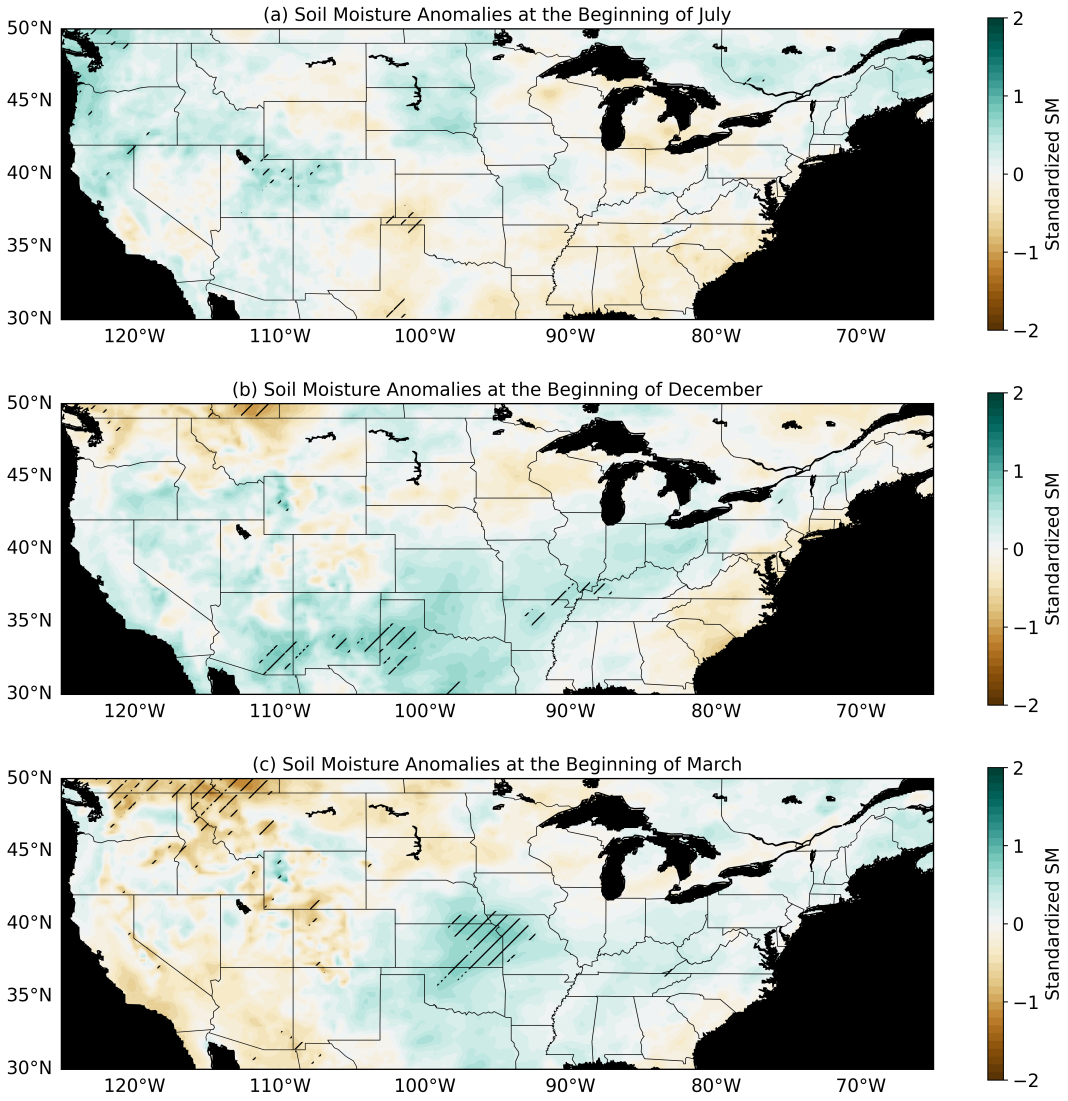

Figure 4.9: Same as Figure 4.8, but for years with a winter La Niña but no July to October AAFD recorded across the region.

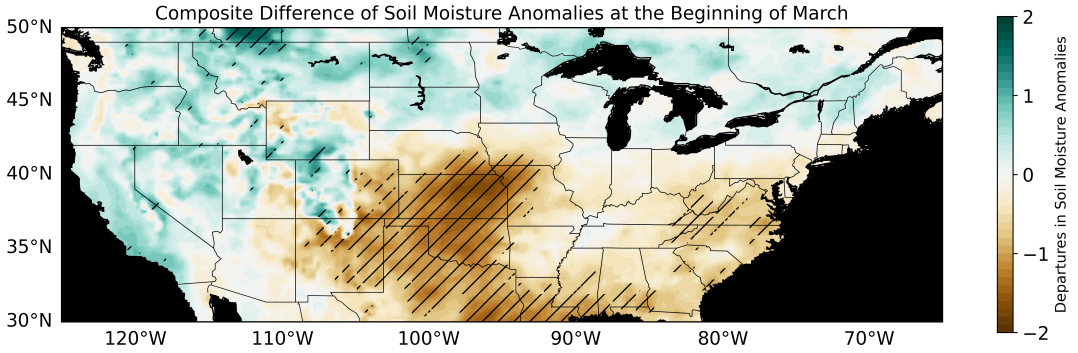

Figure 4.10: Soil moisture anomaly composite difference at the start of March for years following a July-October AAFD and winter La Niña versus years with just a winter La Niña. Hatching indicates regions that have a statistically significant difference in soil moisture anomalies between the 2 data groups, tested to the 95th percentile through bootstrapping (n = 5,000 iterations).

4.2 Midwest

Over the 40-year period of this analysis, results demonstrated that the overall frequency of flash drought within the Midwest peaks during April and May, with a general decline seen into the summer months before a short peak again in October. Further temporal analysis revealed that over the most recent 20-year period, the peak in these events occurred during May, June, and July.

Corn and soybeans are two of the most populated crops across the Midwest region and both crop-growing seasons are illustrated for the state of Iowa in Figures 4.11 and 4.12, respectively. Corn is typically planted in April to early May, whereas soybean planting occurs a few weeks later. Both crops reach maturity during the months of July and August while harvest then takes place from September to November. As a result, an increase in flash drought coverage between the late Spring and Summer months may be highly impactful across this region as it occurs in the early growth and maturing stages of both crops.

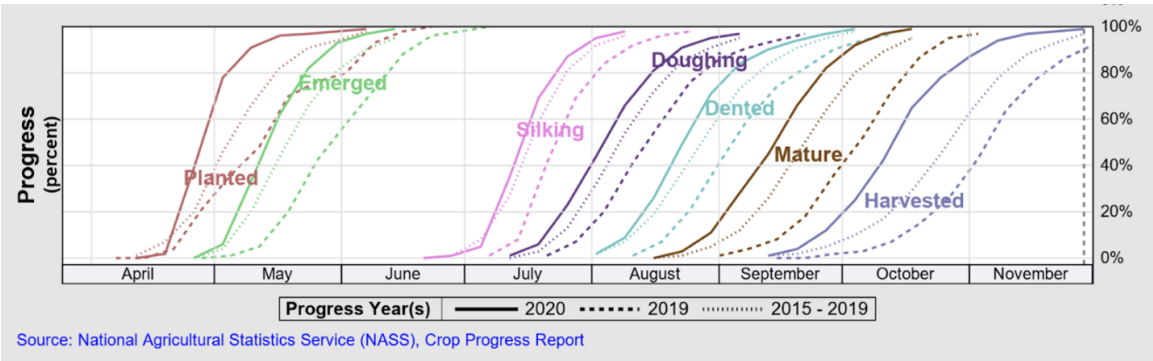

Figure 4.11: Crop growing season calendar for corn in Iowa, including the planting stage (brown lines), emergence (green lines), silking (pink lines), doughing (purple lines), denting (light blue lines), maturity (brown lines) and harvest (periwinkle lines). The solid line (dashed line) represents the timing of corn during the 2020 (2019) growing season. The thinly dashed line represents a five-year average from 2015-2019. (USDA, NASS)

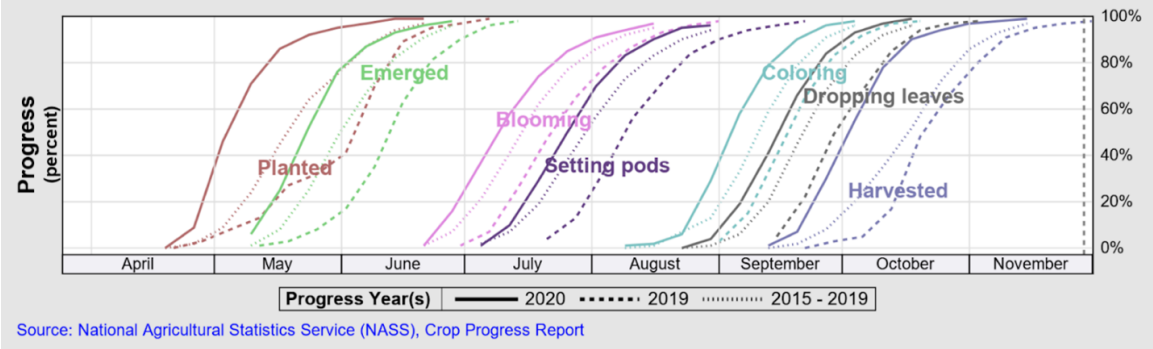

Figure 4.12: Crop growing season calendar for soybeans in Iowa, including the planting stage (brown lines), emergence (green lines), blooming (pink lines), setting pods (purple lines), coloring (light blue lines), dropping leaves (gray lines) and harvest (periwinkle lines). The solid line (dashed line) represents the timing of soybeans during the 2020 (2019) growing season. The thinly dashed line represents a five-year average from 2015-2019. (USDA, NASS)

Further exploration of abrupt flash drought events across the Midwest suggests increased impacts and vulnerability to crops across the region. As seen in Figure 3.11, over 50% more AAFD events affected the Midwest domain from 2001 to 2020 versus those yielded from 1981 to 2000. Further, across the central portion of Iowa, areas experienced 6 to 8 more AAFD events from 2001 to 2020 compared to 1981 to 2000. Analysis of the timing of abrupt flash drought events revealed that more than half of these cases started during April, May, and June.

It is known that prolonged periods of precipitation deficits can aid in the development of flash drought across the Midwest (Basara et al. 2013; Hoerling et al. 2014). In addition to teleconnections causing precipitation fluctuations, significant changes in the yearly distribution of precipitation in the Midwest have been noted. Wang et al. (2015) investigated the seasonal precipitation transition across the central United States, illustrating this significant decrease in rainfall experienced during the early Summer. Moreover, additional analyses focused on trends in this transition show that the precipitation departures are becoming larger across the north-central United States. On the contrary, trends in precipitation departures across the Southern Great Plains are decreasing, indicating that this precipitation change is less intense. These

results provide insight into this peak timing of abrupt flash droughts across the Midwest. Given the Midwest depends on spring rainfall, below-average rainfall during these spring months leaves the ground in a more vulnerable state. Furthermore, if a prolonged period of increased temperatures occurs in the late spring or early summer time frame, increased crop vulnerability to flash drought exists for several reasons. First, precipitation rapidly declines, decreasing the moisture supply of water to the soil. In addition, crops including corn and soybeans have already emerged from the soil. Thus, increased evapotranspiration into the atmosphere will occur from increased plant growth and climatological warming of temperatures. Without precipitation, these factors aid in the desiccation of the ground, which can pose severe impacts, especially given these events occur at key stages in crop development.

Within the Midwest, both soybeans and corn have seen positive trends in their overall yield due to technological advancements (Ling Wang et al. 2018). Nonetheless, abrupt flash drought events can impact crop conditions and overall yield. For example, consider the case of 2003. This event was documented by Hunt et al. (2014) and Chen et al. (2019) and was associated with profound impacts on crop health and overall crop yield productivity at the end of the growing season. Via the AAFD analysis, this event surpassed all 3 criteria and was included in the table of events. Figure A.5 displays the region of the Midwest domain that met all criteria outlined. Figure 4.13 displays the yield productivity expressed in bushels per acre across Iowa from 1981 to 2020 for corn and soybeans, highlighting the yields of corn and soybeans in 2003. Although a significant decline in crop yield was observed for soybeans, a more normal yield was recorded for corn.

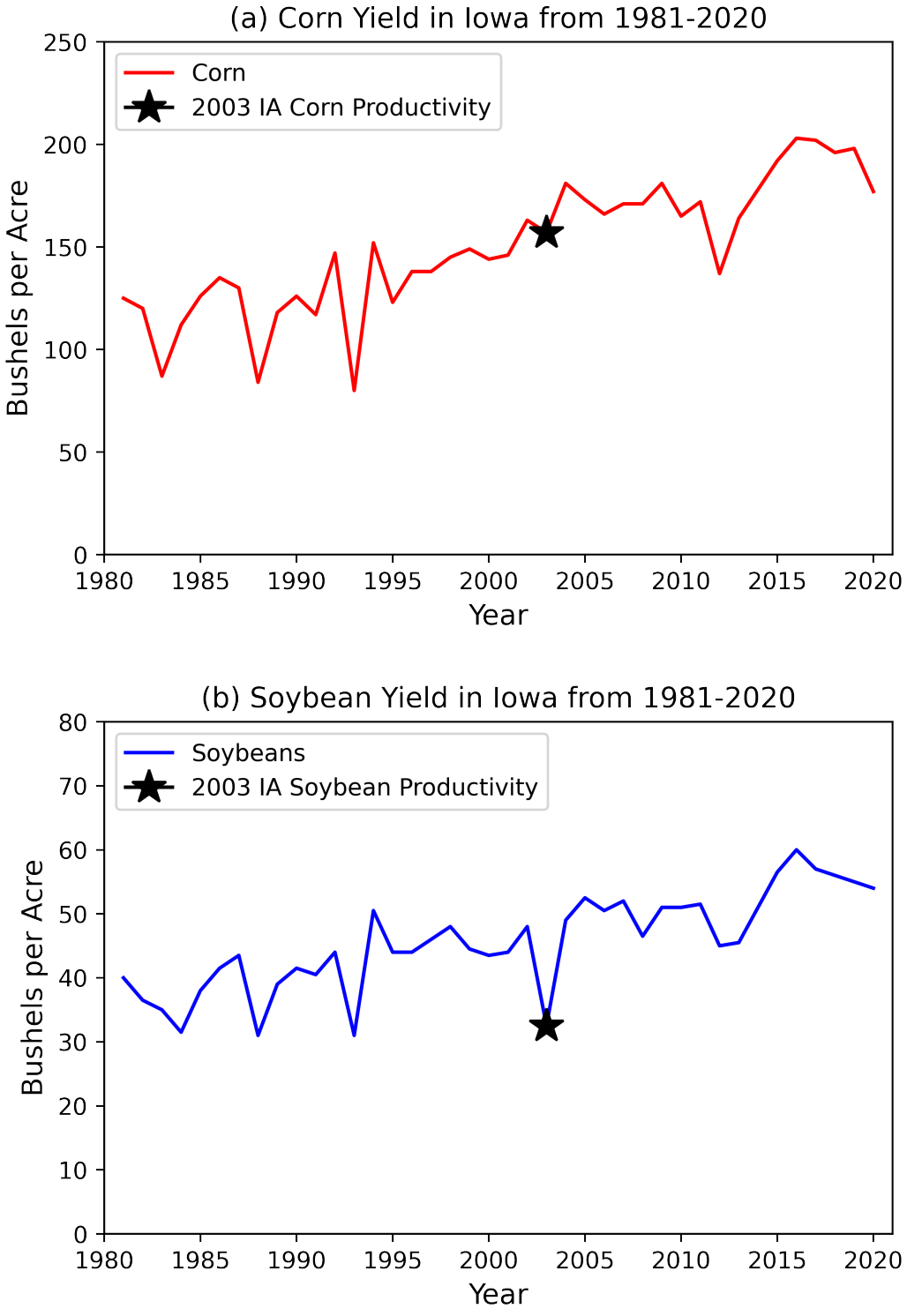

Figure 4.13: (a) Corn yields reported from the USDA NASS for Iowa from 1981 to 2020, expressed in terms of bushels per acre. The black star stippled highlights the corn yield across Iowa in 2003. (b) Same as (a), except for soybeans.

Figure 4.14 displays the evolution of flash drought initialization in 2003 across the Midwest region with the percentage of corn and soybean crops which fell into the category of being either "good" or excellent." Similar to the analysis completed across the Southern Great Plains region, any crop not listed as "excellent" or "good" falls into a category where the expected yield is below normal. This specific abrupt flash drought had a peak initialization into flash drought recorded on July 25. Thus, for at least 30 days across the region, the evaporative demand was significant enough for the region to enter into drought criteria rapidly. During these following weeks of rapid drought intensification, a significant decline was recorded shortly after in the overall crop health of corn and soybeans. By September, both corn and soybean crop conditions had rapidly deteriorated. In two months, the percentage of soybeans listed in "good" or "excellent" condition dropped from 80% to less than 20%. A significant drop in the corn's crop health was also recorded, with a slight recovery noted at the end of the growing season for this crop. At the end of the growing season, while corn saw a slight decrease in crop productivity, soybean productivity dropped by more than 20 percent across the state. The differences in the relative yield of soybeans versus corn during this growing season are likely a result of slightly different growing seasons for each crop. During July and into August, the process of blooming and setting pods occurs with soybeans. It has been shown that drought conditions and high evaporative demand over this time result in some of this crop's most tremendous yield losses (Staton 2020; Wang et al. 2022). Rapid drought transition during this time causes a reduction in the number of seeds, one of the most significant contributors to decreased soybean crop yields in general (Licht and Archontoulis 2017). This AAFD event occurred during one of this crop's most critical growing stages, resulting in the decreased yield productivity observed across the state during 2003.

When assessing the growing stages of corn concerning when this event occurred, this event took place during the doughing stage of the crop. Drought and evaporative stress around the time around silking pose the most significant impacts on crop loss

for corn (Licht and Archontoulis 2017; Heiniger 2018). Given that the silking period ended when the abrupt flash drought initialized across the region, it likely had less of an impact on the overall yield of corn retrieved across the region. Changes were seen to the overall health of this crop; however, the corn crop this year likely was mature enough to remain resilient for a more neutral overall yield.

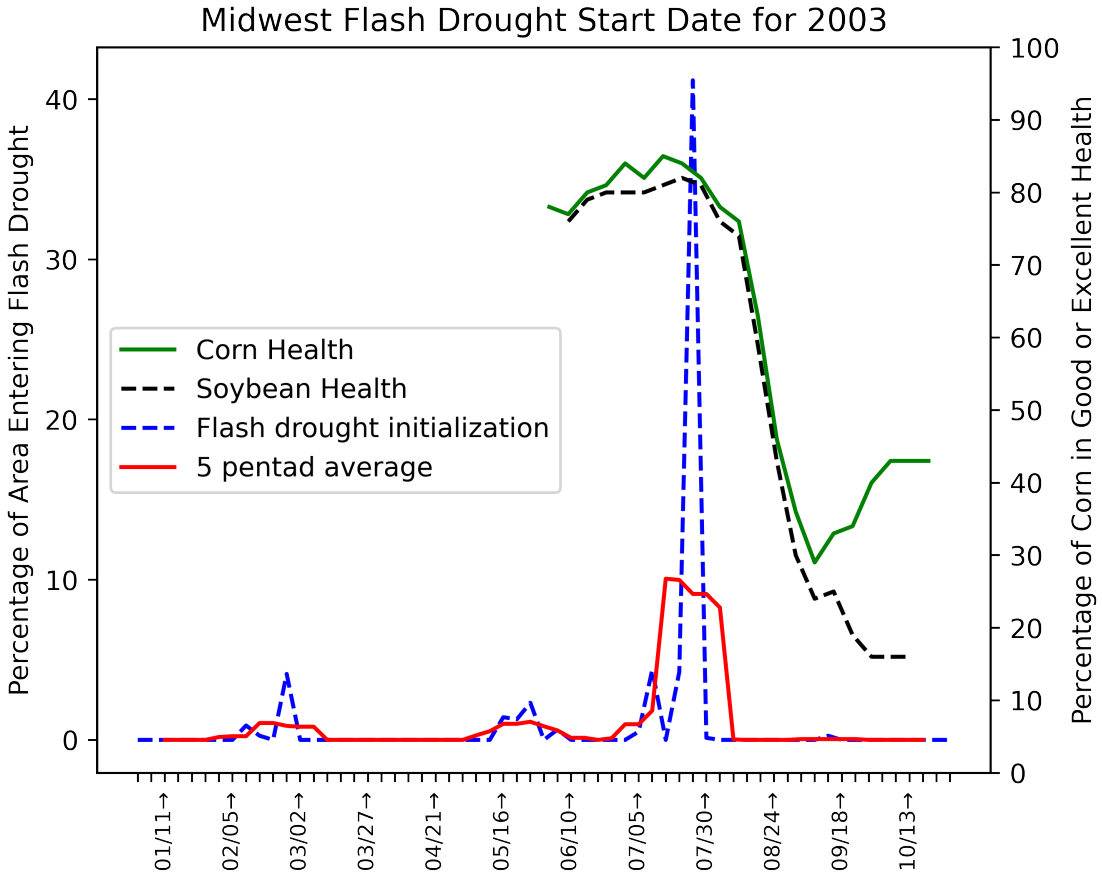

Figure 4.14: Flash drought initialization (blue dashed line) during 2003 across the Midwest region, with a 5-pentad rolling average (red line). The black (green) line represents the percentage of soybeans (corn) that fell into the category of being designated "good" or "excellent."

Chapter 5

Summary and Conclusions

This study presents an analysis of flash drought behavior over two agriculturally dependent regions in the United States. Previous studies (Al-Kaisi et al. 2013; Klemm and McPherson 2018) have confirmed drought impacts both the decision-making process of agricultural producers and the overall yields captured at the end of growing seasons. Via the AAFD definition which examines abrupt flash drought events on a subseasonal to seasonal scale, several important conclusions were made including:

• Across both regions of the United States, there has been an increase in these rapid drought transition events. Specifically, within the Midwest, there was more than a 50% increase in the number of events recorded over the second 20-year period. Moreover, the decade of 2011-2020 recorded almost as many AAFD events compared to the 20-year period from 1981 to 2000.

• Within the Southern Great Plains domain, an increase in rapid drought transition has occurred across much of Oklahoma. Within the Midwest, the highest concentrations of these events were recorded across the central portions of the domain, located over the heart of the corn belt in Iowa.

• In the Southern Great Plains, abrupt flash droughts consistently occurred during almost every month of the defined growing season. Furthermore, a slight peak in events was recorded during the fall months of September and October. This behavior differed significantly from the AAFD events recorded in the Midwest. Within this

region, more than half of the recorded events began between April and June. This concentration of events within this late Spring to early summer time frame is likely tied to the rapid decrease in precipitation experienced during many years across the Midwest domain (Wang et al. 2015). This analysis provides context and understanding of the most vulnerable periods of rapid drought development across the Midwest. Moreover, it conveys as well that these rapid transitions into drought occur most commonly in conjunction with the growing season of crops such as corn and soybeans.

• Across the Southern Great Plains, AAFD events that occur after the harvest of winter wheat (July to October) have a negative effect on crop health and yields the following year when the growing season ends across Texas, Oklahoma, and Kansas. Typically during the fall months, a seasonal increase in soil moisture occurs (Illston et al. 2004), allowing the ground to return to a more moist state for the dormant winter months. When AAFD events occur during this critical period, soil moisture anomalies persist and remain anomalously dry through the winter into the early spring, causing a negative effect on crop health and overall yields. These July-October AAFD events, in conjunction with a winter La Niña pattern, lead to the deterioration of soil moisture, posing a negative impact to the winter wheat crop conditions and yields across Texas, Oklahoma, and Kansas.

• Within the Midwest, a case study of the 2003 abrupt flash drought event showcased the rapid effects flash drought development can pose to the crop health and yields of corn and soybeans. Across the Midwest region, a significant decline in crop health was observed just weeks after the start of AAFD events resulting in major crop losses for soybeans given the AAFD occurred in conjunction with one of the most drought-vulnerable stages for this crop. It was found that corn across this region surpassed a critical maturity stage, resulting in less pronounced crop loss and a relatively normal yield when compared to soybeans. This case study highlights

that the timing of flash drought development on the scale of weeks can pose different effects to crops within the same region based on their distinct growing seasons.

Following the examination of abrupt flash drought behavior across these important regions of agricultural productivity, additional work is needed to gain knowledge of these and similar events as well as event predictability. With two databases of AAFD events for both regions now created, future work can focus on understanding the atmospheric drivers that aid in the development of these events. Case studies have provided sufficient evidence demonstrating that rapidly intensifying drought events can occur from quasi-stationary high-pressure systems which typically results in anomalously warmer temperatures and anomalously less precipitation (Trenberth and Branstator 1992; Hoerling et al. 2014). Given abrupt flash drought timing is unique across the two regions, this suggests that the primary atmospheric drivers for these events are likely different across both regions. Synoptic analysis of atmospheric variables for these events could provide evidence for understanding the atmospheric patterns which favor abrupt flash drought development across the Southern Great Plains versus the Midwest.

Moreover, flash drought events have been recorded in conjunction with other extreme weather events, such as heat waves. For example, the 2010 Russian flash drought was driven by an intense heatwave across Russia which resulted in the deaths of 55,000 people (Hoag 2014). Understanding the relationships between these two subseasonal to seasonal phenomena may provide additional clarity into the prediction of flash drought behavior. Lastly, another vital analysis to be completed following this study would be analyzing the timing of these extreme events in the United States with other extreme events across other portions of the world. For example, during the Summer of 2003, while a significant flash drought developed across the United States, record heat waves were recorded at similar times across Europe and eastern Asia (Bouchama 2004; Huang et al. 2010). Across both Europe and Asia, these

events were directly attributed to the deaths of tens of thousands of humans. Moreover, during the Summer of 2022, a similar situation occurred, as record heatwaves and drought development were recorded across the three same global locations during the same temporal window. Given these events occurred concurrently, analysis of the atmospheric conditions responsible for causing these events in 2003 and 2022 will further our understanding of compound extreme weather events on the sub-seasonal to seasonal scale, and the vulnerability regions may have to abrupt flash drought during these periods.

Reference List

Al-Kaisi, M. M., and Coauthors, 2013: Drought impact on crop production and the soil environment: 2012 experiences from Iowa. *Journal of Soil and Water Conservation*, **68 (1)**, 19A–24A, https://doi.org/10.2489/jswc.68.1.19A, URL http://www.jswconline.org/cgi/doi/10.2489/jswc.68.1.19A.

Allen, R., L. Pereira, D. Raes, and M. Smith, 1998: URL https://www.fao.org/3/x0490e/x0490e06.htm.

Anderson, M. C., C. Hain, B. Wardlow, A. Pimstein, J. R. Mecikalski, and W. P. Kustas, 2011: Evaluation of Drought Indices Based on Thermal Remote Sensing of Evapotranspiration over the Continental United States. *Journal of Climate*, **24 (8)**, 2025–2044, https://doi.org/10.1175/2010JCLI3812.1, URL http://journals.ametsoc.org/doi/10.1175/2010JCLI3812.1.

Basara, J. B., J. I. Christian, R. A. Wakefield, J. A. Otkin, E. H. Hunt, and D. P. Brown, 2019: The evolution, propagation, and spread of flash drought in the Central United States during 2012. *Environmental Research Letters*, **14 (8)**, 084 025, https://doi.org/10.1088/1748-9326/ab2cc0, URL https://iopscience.iop.org/article/10.1088/1748-9326/ab2cc0.

Basara, J. B., J. N. Maybourn, C. M. Peirano, J. E. Tate, P. J. Brown, J. D. Hoey, and B. R. Smith, 2013: Drought and Associated Impacts in the Great Plains of the United States—A Review. *International Journal of Geosciences*, **4 (6)**, 72–81, https://doi.org/10.4236/ijg.2013.46A2009, URL http://www.scirp.org/Journal/Paperabs.aspx?paperid=36204.

Bell, G. D., and J. E. Janowiak, 1995: Atmospheric Circulation Associated with the Midwest Floods of 1993. *Bulletin of the American Meteorological Society*, **76 (5)**, 681–695, https://doi.org/10.1175/1520-0477(1995)076⟨0681:ACAWTM⟩2.0.CO;2, URL http://journals.ametsoc.org/doi/10.1175/1520-0477(1995)076⟨0681:ACAWTM⟩2.0.CO;2.

Bouchama, A., 2004: The 2003 European heat wave. *Intensive Care Medicine*, **30 (1)**, 1–3, https://doi.org/10.1007/s00134-003-2062-y, URL http://link.springer.com/10.1007/s00134-003-2062-y.

Changnon, S. A., 1989: The 1988 Drought, Barges, and Diversion. *Bulletin of the American Meteorological Society*, **70 (9)**, 1092–1104, https://doi.org/10.1175/1520-0477(1989)070⟨1092:TDBAD⟩2.0.CO;2, URL http://journals.ametsoc.org/doi/10.1175/1520-0477(1989)070⟨1092:TDBAD⟩2.0.CO;2.

Chen, J., P. Jönsson, M. Tamura, Z. Gu, B. Matsushita, and L. Eklundh, 2004: A simple method for reconstructing a high-quality NDVI time-series data set based

on the Savitzky–Golay filter. *Remote Sensing of Environment*, **91 (3-4)**, 332–344, https://doi.org/10.1016/j.rse.2004.03.014, URL https://linkinghub.elsevier.com/retrieve/pii/S003442570400080X.

Chen, L. G., J. Gottschalck, A. Hartman, D. Miskus, R. Tinker, and A. Artusa, 2019: Flash Drought Characteristics Based on U.S. Drought Monitor. *Atmosphere*, **10 (9)**, 498, https://doi.org/10.3390/atmos10090498, URL https://www.mdpi.com/2073-4433/10/9/498.

Christian, J. I., J. B. Basara, E. D. Hunt, J. A. Otkin, J. C. Furtado, V. Mishra, X. Xiao, and R. M. Randall, 2021: Global distribution, trends, and drivers of flash drought occurrence. *Nature Communications*, **12 (1)**, 6330, https://doi.org/10.1038/s41467-021-26692-z, URL https://www.nature.com/articles/s41467-021-26692-z.

Christian, J. I., J. B. Basara, E. D. Hunt, J. A. Otkin, and X. Xiao, 2020: Flash drought development and cascading impacts associated with the 2010 Russian heatwave. *Environmental Research Letters*, **15 (9)**, 094 078, https://doi.org/10.1088/1748-9326/ab9faf, URL https://iopscience.iop.org/article/10.1088/1748-9326/ab9faf.

Christian, J. I., J. B. Basara, L. E. L. Lowman, X. Xiao, D. Mesheske, and Y. Zhou, 2022: Flash drought identification from satellite-based land surface water index. *Remote Sensing Applications: Society and Environment*, **26**, 100 770, https://doi.org/10.1016/j.rsase.2022.100770, URL https://www.sciencedirect.com/science/article/pii/S2352938522000787.

Christian, J. I., J. B. Basara, J. A. Otkin, and E. D. Hunt, 2019a: Regional characteristics of flash droughts across the United States. *Environmental Research Communications*, **1 (12)**, 125 004, https://doi.org/10.1088/2515-7620/ab50ca, URL https://iopscience.iop.org/article/10.1088/2515-7620/ab50ca.

Christian, J. I., J. B. Basara, J. A. Otkin, E. D. Hunt, R. A. Wakefield, P. X. Flanagan, and X. Xiao, 2019b: A Methodology for Flash Drought Identification: Application of Flash Drought Frequency across the United States. *Journal of Hydrometeorology*, **20 (5)**, 833–846, https://doi.org/10.1175/JHM-D-18-0198.1, URL http://journals.ametsoc.org/doi/10.1175/JHM-D-18-0198.1.

Climate Prediction Center, 2023: Climate Prediction Center. URL https://www.cpc.ncep.noaa.gov/.

Dai, A., 2013: Increasing drought under global warming in observations and models. *Nature Climate Change*, **3 (1)**, 52–58, https://doi.org/10.1038/nclimate1633, URL https://www.nature.com/articles/nclimate1633.

dos Santos, C. A. C., C. M. U. Neale, M. M. Mekonnen, I. Z. Gonçalves, G. de Oliveira, O. Ruiz-Alvarez, B. Safa, and C. M. Rowe, 2022: Trends of extreme air temperature and precipitation and their impact on corn and soybean yields in Nebraska,

USA. *Theoretical and Applied Climatology*, **147 (3)**, 1379–1399, https://doi.org/10.1007/s00704-021-03903-7, URL https://doi.org/10.1007/s00704-021-03903-7.

Eck, M. A., A. R. Murray, A. R. Ward, and C. E. Konrad, 2020: Influence of growing season temperature and precipitation anomalies on crop yield in the southeastern United States. *Agricultural and Forest Meteorology*, **291**, 108 053, https://doi.org/10.1016/j.agrformet.2020.108053, URL https://linkinghub.elsevier.com/retrieve/pii/S0168192320301556.

Edris, S. G., J. B. Basara, J. I. Christian, E. D. Hunt, J. A. Otkin, S. T. Salesky, and B. G. Illston, 2022: Decomposing the Critical Components of Flash Drought Using the Standardized Evaporative Stress Ratio. Rochester, NY, URL https://papers.ssrn.com/abstract=4136023, https://doi.org/10.2139/ssrn.4136023.

Flanagan, P. X., J. B. Basara, J. C. Furtado, E. R. Martin, and X. Xiao, 2019: Role of Sea Surface Temperatures in Forcing Circulation Anomalies Driving U.S. Great Plains Pluvial Years. *Journal of Climate*, **32 (20)**, 7081–7100, https://doi.org/10.1175/JCLI-D-18-0726.1, URL http://journals.ametsoc.org/doi/10.1175/JCLI-D-18-0726.1.

Flanagan, P. X., J. B. Basara, B. G. Illston, and J. A. Otkin, 2017: The Effect of the Dry Line and Convective Initiation on Drought Evolution over Oklahoma during the 2011 Drought. *Advances in Meteorology*, **2017**, 1–16, https://doi.org/10.1155/2017/8430743, URL https://www.hindawi.com/journals/amete/2017/8430743/.

Ford, T. W., D. B. McRoberts, S. M. Quiring, and R. E. Hall, 2015: On the utility of in situ soil moisture observations for flash drought early warning in Oklahoma, USA: SOIL MOISTURE DROUGHT EARLY WARNING. *Geophysical Research Letters*, **42 (22)**, 9790–9798, https://doi.org/10.1002/2015GL066600, URL http://doi.wiley.com/10.1002/2015GL066600.

Granger, R., 1989: An examination of the concept of potential evaporation. *Journal of Hydrology*, **111 (1-4)**, 9–19, https://doi.org/10.1016/0022-1694(89)90248-5, URL https://linkinghub.elsevier.com/retrieve/pii/0022169489902485.

He, M., J. S. Kimball, Y. Yi, S. Running, K. Guan, K. Jensco, B. Maxwell, and M. Maneta, 2019: Impacts of the 2017 flash drought in the US Northern plains informed by satellite-based evapotranspiration and solar-induced fluorescence. *Environmental Research Letters*, **14 (7)**, 074 019, https://doi.org/10.1088/1748-9326/ab22c3, URL https://dx.doi.org/10.1088/1748-9326/ab22c3.

Heiniger, R., 2018: The Impact of Early Drought on Corn Yield. Tech. rep, North Carolina State Extension. https://corn.ces.ncsu.edu/corn-production-information/the-impact-of-early-drought-on-corn-yield/.

Hersbach, H., and Coauthors, 2020: The ERA5 global reanalysis. *Quarterly Journal of the Royal Meteorological Society*, **146 (730)**, 1999–2049, https://doi.org/10.1002/qj.3803, URL https://onlinelibrary.wiley.com/doi/10.1002/qj.3803.

Hoag, H., 2014: Russian summer tops 'universal' heatwave index. *Nature*, nature.2014.16250, https://doi.org/10.1038/nature.2014.16250, URL http://www.nature.com/articles/nature.2014.16250.

Hobbins, M. T., A. Wood, D. J. McEvoy, J. L. Huntington, C. Morton, M. Anderson, and C. Hain, 2016: The Evaporative Demand Drought Index. Part I: Linking Drought Evolution to Variations in Evaporative Demand. *Journal of Hydrometeorology*, **17 (6)**, 1745–1761, https://doi.org/10.1175/JHM-D-15-0121.1, URL http://journals.ametsoc.org/doi/10.1175/JHM-D-15-0121.1.

Hoell, A., and Coauthors, 2020: Lessons Learned from the 2017 Flash Drought across the U.S. Northern Great Plains and Canadian Prairies. *Bulletin of the American Meteorological Society*, **101 (12)**, E2171–E2185, https://doi.org/10.1175/BAMS-D-19-0272.1, URL https://journals.ametsoc.org/view/journals/bams/101/12/BAMS-D-19-0272.1.xml.

Hoerling, M., J. Eischeid, A. Kumar, R. Leung, A. Mariotti, K. Mo, S. Schubert, and R. Seager, 2014: Causes and Predictability of the 2012 Great Plains Drought. *Bulletin of the American Meteorological Society*, **95 (2)**, 269–282, https://doi.org/10.1175/BAMS-D-13-00055.1, URL https://journals.ametsoc.org/view/journals/bams/95/2/bams-d-13-00055.1.xml.

Huang, W., H. Kan, and S. Kovats, 2010: The impact of the 2003 heat wave on mortality in Shanghai, China. *Science of The Total Environment*, **408 (11)**, 2418–2420, https://doi.org/10.1016/j.scitotenv.2010.02.009, URL https://linkinghub.elsevier.com/retrieve/pii/S0048969710001208.

Hunt, E., and Coauthors, 2021: Agricultural and food security impacts from the 2010 Russia flash drought. *Weather and Climate Extremes*, **34**, 100 383, https://doi.org/10.1016/j.wace.2021.100383, URL https://linkinghub.elsevier.com/retrieve/pii/S2212094721000736.

Hunt, E. D., M. Svoboda, B. Wardlow, K. Hubbard, M. Hayes, and T. Arkebauer, 2014: Monitoring the effects of rapid onset of drought on non-irrigated maize with agronomic data and climate-based drought indices. *Agricultural and Forest Meteorology*, **191**, 1–11, https://doi.org/10.1016/j.agrformet.2014.02.001, URL https://linkinghub.elsevier.com/retrieve/pii/S0168192314000409.

Illston, B. G., J. B. Basara, and K. C. Crawford, 2004: Seasonal to interannual variations of soil moisture measured in Oklahoma. *International Journal of Climatology*, **24 (15)**, 1883–1896, https://doi.org/10.1002/joc.1077, URL https://onlinelibrary.wiley.com/doi/10.1002/joc.1077.

Jin, C., X. Luo, X. Xiao, J. Dong, X. Li, J. Yang, and D. Zhao, 2019: The 2012 Flash Drought Threatened US Midwest Agroecosystems. *Chinese Geographical Science*, **29 (5)**, 768–783, https://doi.org/10.1007/s11769-019-1066-7, URL http://link.springer.com/10.1007/s11769-019-1066-7.

Kansas State College of Agriculture and Applied Science, 1936: Agricultural Experiment Station. Tech. rep., Manhattan, Kansas. URL https://www.ksre.k-state.edu/historicpublications/pubs/SB273.pdf.

Klemm, T., and R. A. McPherson, 2018: Assessing Decision Timing and Seasonal Climate Forecast Needs of Winter Wheat Producers in the South-Central United States. *Journal of Applied Meteorology and Climatology*, **57 (9)**, 2129–2140, https://doi.org/10.1175/JAMC-D-17-0246.1, URL https://journals.ametsoc.org/view/journals/apme/57/9/jamc-d-17-0246.1.xml.

Koster, R. D., S. D. Schubert, H. Wang, S. P. Mahanama, and A. M. DeAngelis, 2019: Flash Drought as Captured by Reanalysis Data: Disentangling the Contributions of Precipitation Deficit and Excess Evapotranspiration. *Journal of Hydrometeorology*, **20 (6)**, 1241–1258, https://doi.org/10.1175/JHM-D-18-0242.1, URL http://journals.ametsoc.org/doi/10.1175/JHM-D-18-0242.1.

Li, J., Z. Wang, X. Wu, S. Guo, and X. Chen, 2020: Flash droughts in the Pearl River Basin, China: Observed characteristics and future changes. *Science of The Total Environment*, **707**, 136 074, https://doi.org/10.1016/j.scitotenv.2019.136074, URL https://linkinghub.elsevier.com/retrieve/pii/S004896971936070X.

Licht, M., and S. Archontoulis, 2017: Influence of Drought on Corn and Soybean. URL https://crops.extension.iastate.edu/cropnews/2017/07/influence-drought-corn-and-soybean.

Ling Wang, S., R. Nehring, and R. Mosheim, 2018: Agrticultural Productivity Growth in the United States: 1948-2015. Tech. rep., US Department of Agriculture, Economic Research Service. URL https://www.ers.usda.gov/amber-waves/2018/march/agricultural-productivity-growth-in-the-united-states-1948-2015/).

Lisonbee, J., J. Ribbe, J. A. Otkin, and C. Pudmenzky, 2022: Wet season rainfall onset and flash drought: The case of the northern Australian wet season. *International Journal of Climatology*, **42 (12)**, 6499–6514, https://doi.org/10.1002/joc.7609, URL https://onlinelibrary.wiley.com/doi/10.1002/joc.7609.

Lisonbee, J., M. Woloszyn, and M. Skumanich, 2021: Making sense of flash drought: definitions, indicators, and where we go from here. *Journal of Applied and Service Climatology*, **2021 (1)**, 1–19, https://doi.org/10.46275/JOASC.2021.02.001, URL https://stateclimate.org/pdfs/journal-articles/2021_1-Lisonbee.pdf.

Lollato, R. P., J. T. Edwards, and T. E. Ochsner, 2017: Meteorological limits to winter wheat productivity in the U.S. southern Great Plains. *Field Crops Research*, **203**, 212–226, https://doi.org/10.1016/j.fcr.2016.12.014, URL https://www.sciencedirect.com/science/article/pii/S037842901630870X.

Mauget, S. A., and D. R. Upchurch, 1999: El Niño and La Niña Related Climate and Agricultural Impacts over the Great Plains and Midwest. *Journal of Production Agriculture*, **12 (2)**, 203–215, https://doi.org/10.2134/jpa1999.0203, URL http://doi.wiley.com/10.2134/jpa1999.0203.

Mo, K. C., and D. P. Lettenmaier, 2016: Precipitation Deficit Flash Droughts over the United States. *Journal of Hydrometeorology*, **17 (4)**, 1169–1184, https://doi.org/10.1175/JHM-D-15-0158.1, URL http://journals.ametsoc.org/doi/10.1175/JHM-D-15-0158.1.

Mo, K. C., and D. P. Lettenmaier, 2020: Prediction of Flash Droughts over the United States. *Journal of Hydrometeorology*, **21 (8)**, 1793–1810, https://doi.org/10.1175/JHM-D-19-0221.1, URL https://journals.ametsoc.org/view/journals/hydr/21/8/jhmD190221.xml.

Nguyen, H., M. C. Wheeler, J. A. Otkin, T. Cowan, A. Frost, and R. Stone, 2019: Using the evaporative stress index to monitor flash drought in Australia. *Environmental Research Letters*, **14 (6)**, 064 016, https://doi.org/10.1088/1748-9326/ab2103, URL https://iopscience.iop.org/article/10.1088/1748-9326/ab2103.

NOAA, NCEI, 2009: Climate Variability: Oceanic Niño Index | NOAA Climate.gov. URL https://www.climate.gov/news-features/understanding-climate/climate-variability-oceanic-ni\%C3\%B1o-index.

Otkin, J. A., M. C. Anderson, C. Hain, I. E. Mladenova, J. B. Basara, and M. Svoboda, 2013: Examining Rapid Onset Drought Development Using the Thermal Infrared–Based Evaporative Stress Index. *Journal of Hydrometeorology*, **14 (4)**, 1057–1074, https://doi.org/10.1175/JHM-D-12-0144.1, URL http://journals.ametsoc.org/doi/10.1175/JHM-D-12-0144.1.

Otkin, J. A., M. Shafer, M. Svoboda, B. Wardlow, M. C. Anderson, C. Hain, and J. Basara, 2015: Facilitating the Use of Drought Early Warning Information through Interactions with Agricultural Stakeholders. *Bulletin of the American Meteorological Society*, **96 (7)**, 1073–1078, https://doi.org/10.1175/BAMS-D-14-00219.1, URL https://journals.ametsoc.org/doi/10.1175/BAMS-D-14-00219.1.

Otkin, J. A., M. Svoboda, E. D. Hunt, T. W. Ford, M. C. Anderson, C. Hain, and J. B. Basara, 2018: Flash Droughts: A Review and Assessment of the Challenges Imposed by Rapid-Onset Droughts in the United States. *Bulletin of the American Meteorological Society*, **99 (5)**, 911–919, https://doi.org/10.1175/BAMS-D-17-0149.1, URL https://journals.ametsoc.org/view/journals/bams/99/5/bams-d-17-0149.1.xml.

Parker, T., A. Gallant, M. Hobbins, and D. Hoffmann, 2021: Flash drought in Australia and its relationship to evaporative demand. *Environmental Research Letters*, **16 (6)**, 064 033, https://doi.org/10.1088/1748-9326/abfe2c, URL https://iopscience.iop.org/article/10.1088/1748-9326/abfe2c.

Pendergrass, A. G., and Coauthors, 2020: Flash droughts present a new challenge for subseasonal-to-seasonal prediction. *Nature Climate Change*, **10 (3)**, 191–199, https://doi.org/10.1038/s41558-020-0709-0.

Pereira, L. S., A. Perrier, R. G. Allen, and I. Alves, 1999: Evapotranspiration: Concepts and Future Trends. *Journal of Irrigation and Drainage Engineering*, **125 (2)**, 45–51, https://doi.org/10.1061/(ASCE)0733-9437(1999)125:2(45), URL https://ascelibrary.org/doi/10.1061/\%28ASCE\%290733-9437\%281999\%29125\%3A2\%2845\%29.

Peters, A. J., E. A. Walter-Shea, L. Ji, A. Viña, M. Hayes, and M. D. Svoboda, 2002: Drought monitoring with NDVI-based Standardized Vegetation Index. *Photogramm Eng*, **68 (1)**, 71–75, URL http://www.scopus.com/inward/record.url?scp=0036155911&partnerID=8YFLogxK.

Pu, B., R. Fu, R. E. Dickinson, and D. N. Fernando, 2016: Why do summer droughts in the Southern Great Plains occur in some La Niña years but not others?: DROUGHTS IN THE SOUTHERN GREAT PLAINS. *Journal of Geophysical Research: Atmospheres*, **121 (3)**, 1120–1137, https://doi.org/10.1002/2015JD023508, URL http://doi.wiley.com/10.1002/2015JD023508.

Qing, Y., S. Wang, B. C. Ancell, and Z.-L. Yang, 2022: Accelerating flash droughts induced by the joint influence of soil moisture depletion and atmospheric aridity. *Nature Communications*, **13 (1)**, 1139, https://doi.org/10.1038/s41467-022-28752-4, URL https://www.nature.com/articles/s41467-022-28752-4.

Rippey, B. R., 2015: The U.S. drought of 2012. *Weather and Climate Extremes*, **10**, 57–64, https://doi.org/10.1016/j.wace.2015.10.004, URL https://www.sciencedirect.com/science/article/pii/S2212094715300360.

Sacks, W. J., D. Deryng, J. A. Foley, and N. Ramankutty, 2010: Crop planting dates: an analysis of global patterns: Global crop planting dates. *Global Ecology and Biogeography*, no–no, https://doi.org/10.1111/j.1466-8238.2010.00551.x, URL https://onlinelibrary.wiley.com/doi/10.1111/j.1466-8238.2010.00551.x.

Salley, S. W., R. O. Sleezer, R. M. Bergstrom, P. H. Martin, and E. F. Kelly, 2016: A long-term analysis of the historical dry boundary for the Great Plains of North America: Implications of climatic variability and climatic change on temporal and spatial patterns in soil moisture. *Geoderma*, **274**, 104–113, https://doi.org/10.1016/j.geoderma.2016.03.020, URL https://www.sciencedirect.com/science/article/pii/S0016706116301380.

Seager, R., N. Lis, J. Feldman, M. Ting, A. P. Williams, J. Nakamura, H. Liu, and N. Henderson, 2018: Whither the 100th Meridian? The Once and Future Physical and Human Geography of America's Arid–Humid Divide. Part I: The Story So Far. *Earth Interactions*, **22 (5)**, 1–22, https://doi.org/10.1175/EI-D-17-0011.1, URL https://journals.ametsoc.org/doi/10.1175/EI-D-17-0011.1.

Sentelhas, P. C., T. J. Gillespie, and E. A. Santos, 2010: Evaluation of FAO Penman–Monteith and alternative methods for estimating reference evapotranspiration with missing data in Southern Ontario, Canada. *Agricultural Water Management*, **97 (5)**, 635–644, https://doi.org/10.1016/j.agwat.2009.12.001, URL https://www.sciencedirect.com/science/article/pii/S0378377409003436.

Shabbar, A., and B. Yu, 2009: The 1998–2000 La Niña in the context of historically strong La Niña events. *Journal of Geophysical Research*, **114 (D13)**, D13 105, https://doi.org/10.1029/2008JD011185, URL http://doi.wiley.com/10.1029/2008JD011185.

Staton, M., 2020: Moisture stress and high temperature effects on soybean yields. URL https://www.canr.msu.edu/news/moisture_stress_and_high_temperature_effects_on_soybean_yields.

Svoboda, M., and Coauthors, 2002: THE DROUGHT MONITOR. *Bulletin of the American Meteorological Society*, **83 (8)**, 1181–1190, https://doi.org/10.1175/1520-0477-83.8.1181, URL https://journals.ametsoc.org/doi/10.1175/1520-0477-83.8.1181.

Sánchez, N., González-Zamora, M. Piles, and J. Martínez-Fernández, 2016: A New Soil Moisture Agricultural Drought Index (SMADI) Integrating MODIS and SMOS Products: A Case of Study over the Iberian Peninsula. *Remote Sensing*, **8 (4)**, 287, https://doi.org/10.3390/rs8040287, URL http://www.mdpi.com/2072-4292/8/4/287.

Trenberth, K. E., 1997: The Definition of El Niño. *Bulletin of the American Meteorological Society*, **78 (12)**, 2771–2777, https://doi.org/10.1175/1520-0477(1997)078⟨2771:TDOENO⟩2.0.CO;2, URL http://journals.ametsoc.org/doi/10.1175/1520-0477(1997)078⟨2771:TDOENO⟩2.0.CO;2.

Trenberth, K. E., and G. W. Branstator, 1992: Issues in Establishing Causes of the 1988 Drought over North America. *Journal of Climate*, **5 (2)**, 159–172, https://doi.org/10.1175/1520-0442(1992)005⟨0159:IIECOT⟩2.0.CO;2, URL https://journals.ametsoc.org/view/journals/clim/5/2/1520-0442_1992_005_0159_iiecot_2_0_co_2.xml.

Trenberth, K. E., and D. P. Stepaniak, 2001: Indices of El Niño Evolution. *Journal of Climate*, **14 (8)**, 1697–1701, https://doi.org/10.1175/1520-0442(2001)014⟨1697:LIOENO⟩2.0.CO;2, URL http://journals.ametsoc.org/doi/10.1175/1520-0442(2001)014⟨1697:LIOENO⟩2.0.CO;2.

University of Minnesota, 2023: Biodiversity and Productivity Has Grown in Modern U.S. Wheat Varieties. URL https://www.uswheat.org/wheatletter/biodiversity-and-productivity-has-grown-in-modern-u-s-wheat-varieties/.

USDA, Economic Research Service, 2015: U.S. Drought 2012: Farm and Food Impacts. Tech. rep. URL https://drought.unl.edu/archive/assessments/USDA-ERS-2012-farm-food-impacts.pdf.

USDA, Farm Service Agency, 2020: Secretarial Disaster Designations for Drought.

USDA, NASS, 2022: July Crop Production. Tech. rep. URL https://www.nass.usda.gov/Statistics_by_State/Oklahoma/Publications/Recent_Reports/2022/spr-crop-prod-07-2022.pdf.

Vogel, F. A., G. A. Bange, F. A. Vogel, and G. A. Bange, 1999: Understanding USDA Crop Forecasts. https://doi.org/10.22004/AG.ECON.320799, URL https://ageconsearch.umn.edu/record/320799.

Wang, S. S., and Coauthors, 2015: An intensified seasonal transition in the Central U.S. that enhances summer drought. *Journal of Geophysical Research: Atmospheres*, **120 (17)**, 8804–8816, https://doi.org/10.1002/2014JD023013, URL https://onlinelibrary.wiley.com/doi/abs/10.1002/2014JD023013.

Wang, X., Z. Wu, Q. Zhou, X. Wang, S. Song, and S. Dong, 2022: Physiological Response of Soybean Plants to Water Deficit. *Frontiers in Plant Science*, **12**, 809 692, https://doi.org/10.3389/fpls.2021.809692, URL https://www.frontiersin.org/articles/10.3389/fpls.2021.809692/full.

Woli, P., B. V. Ortiz, J. Johnson, and G. Hoogenboom, 2015: El Niño–Southern Oscillation Effects on Winter Wheat in the Southeastern United States. *Agronomy Journal*, **107 (6)**, 2193–2204, https://doi.org/10.2134/agronj14.0651, URL https://onlinelibrary.wiley.com/doi/10.2134/agronj14.0651.

Xu, Z.-g., Z.-y. Wu, H. He, X. Guo, and Y.-l. Zhang, 2021: Comparison of soil moisture at different depths for drought monitoring based on improved soil moisture anomaly percentage index. *Water Science and Engineering*, **14 (3)**, 171–183, https://doi.org/10.1016/j.wse.2021.08.008, URL https://linkinghub.elsevier.com/retrieve/pii/S1674237021000806.

Zhao, H., and Coauthors, 2022: U.S. winter wheat yield loss attributed to compound hot-dry-windy events. *Nature Communications*, **13 (1)**, 7233, https://doi.org/10.1038/s41467-022-34947-6, URL https://www.nature.com/articles/s41467-022-34947-6.

Zipper, S. C., J. Qiu, and C. J. Kucharik, 2016: Drought effects on US maize and soybean production: spatiotemporal patterns and historical changes. *Environmental Research Letters*, **11 (9)**, 094 021, https://doi.org/10.1088/1748-9326/11/9/094021, URL https://dx.doi.org/10.1088/1748-9326/11/9/094021.

1 Appendixed Images and Tables

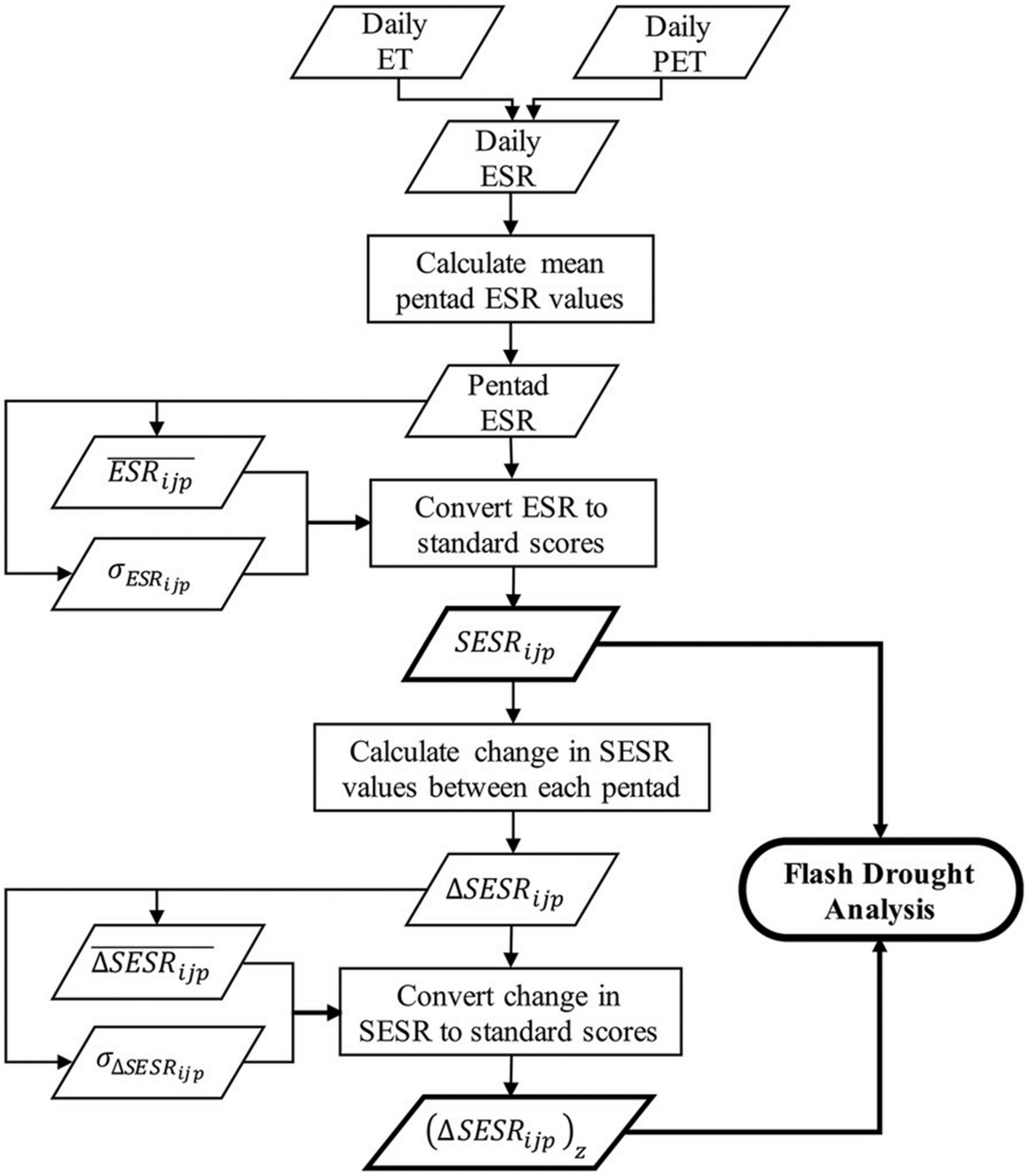

Figure A.1: Flowchart illustrating the pentad-based calculation of the standardized evaporative stress ratio (SESR). This figure is taken from Christian et al. (2019b).

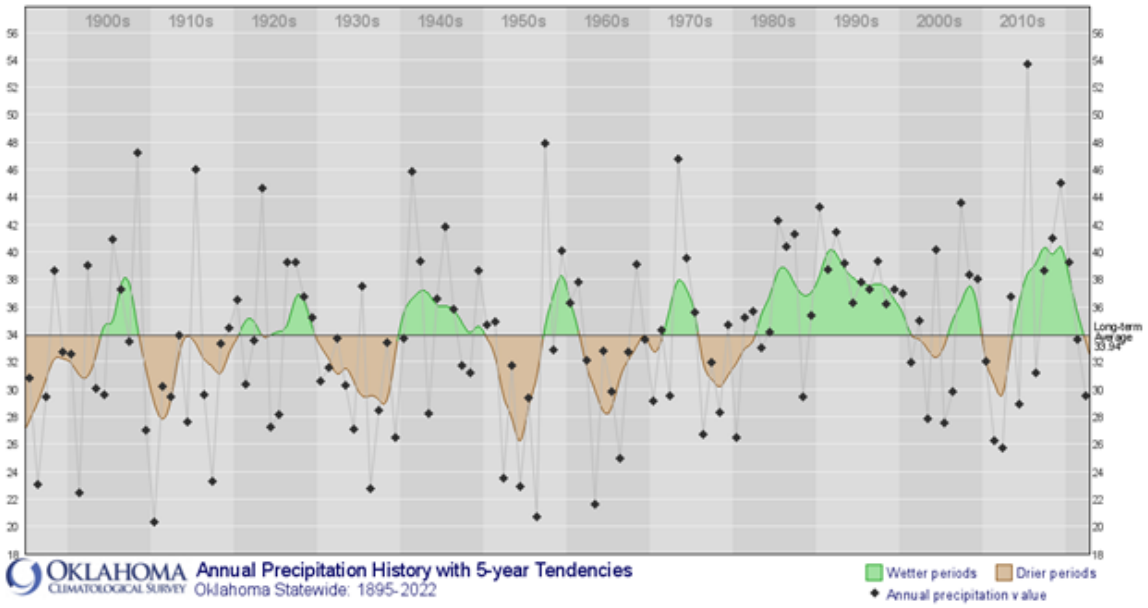

Figure A.2: Yearly averaged precipitation (black dots) across Oklahoma from 1895 to 2022. The smoothed line represents a 5-year weighted average (Oklahoma Climatological Survey, 2023).

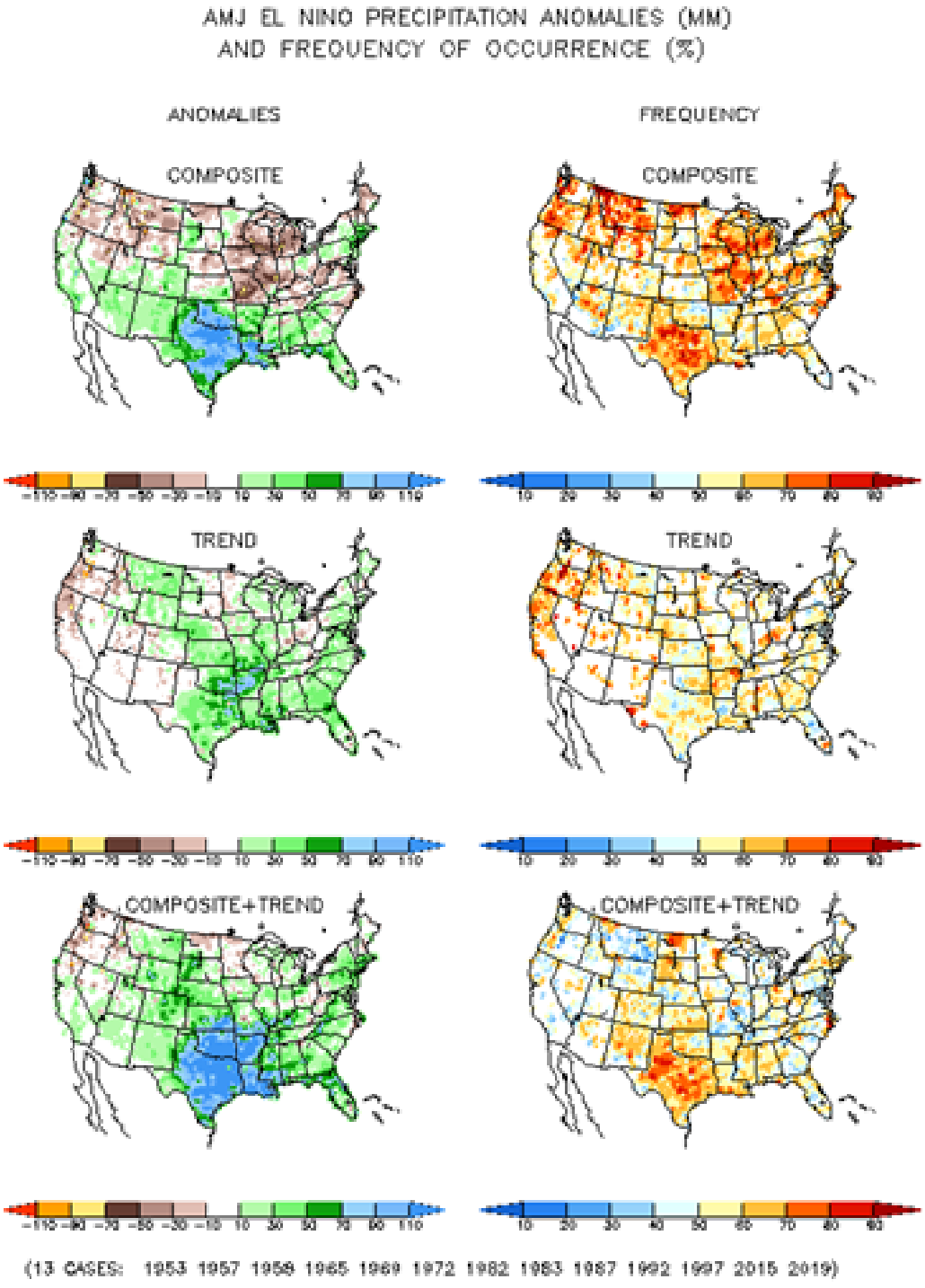

Figure A.3: Average precipitation anomalies experienced across the continental United States during El Niño regimes from April to June. The years included in this figure all had El Niño signals over these months from 1950 to present day. (Climate Prediction Center, CPC)

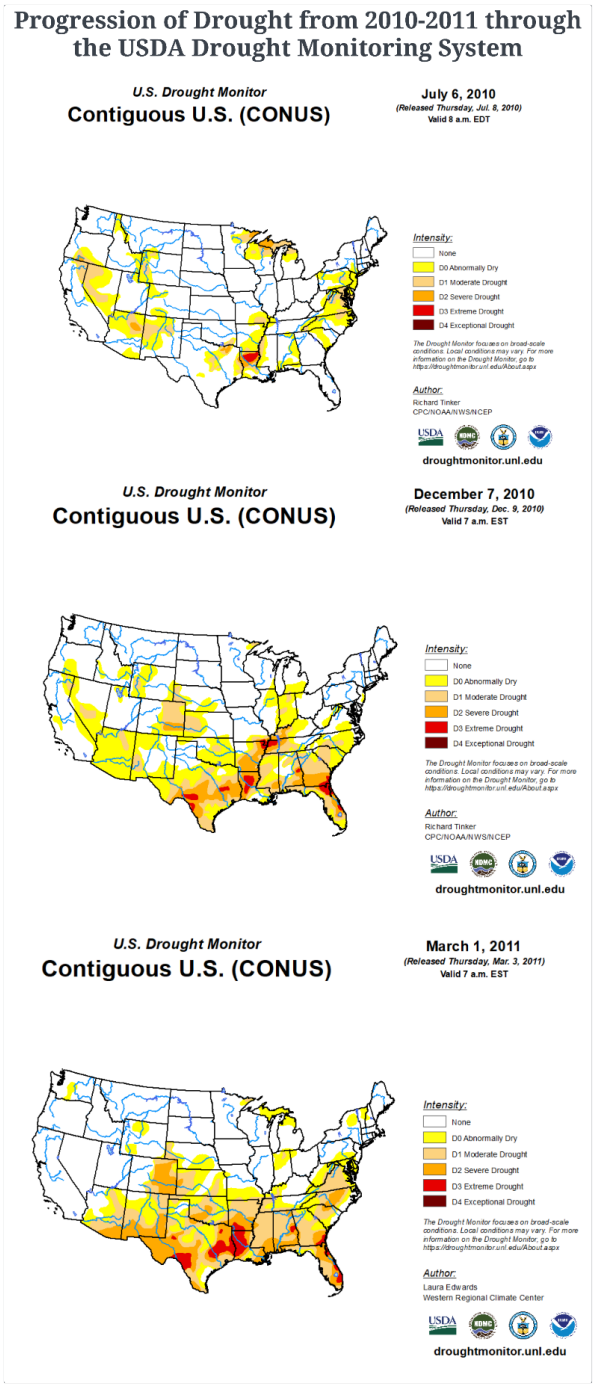

Figure A.4: United States Drought Monitor map at three points in time: (a) July 6, 2010; (b) December 7, 2010; and (c) March 1, 2011.

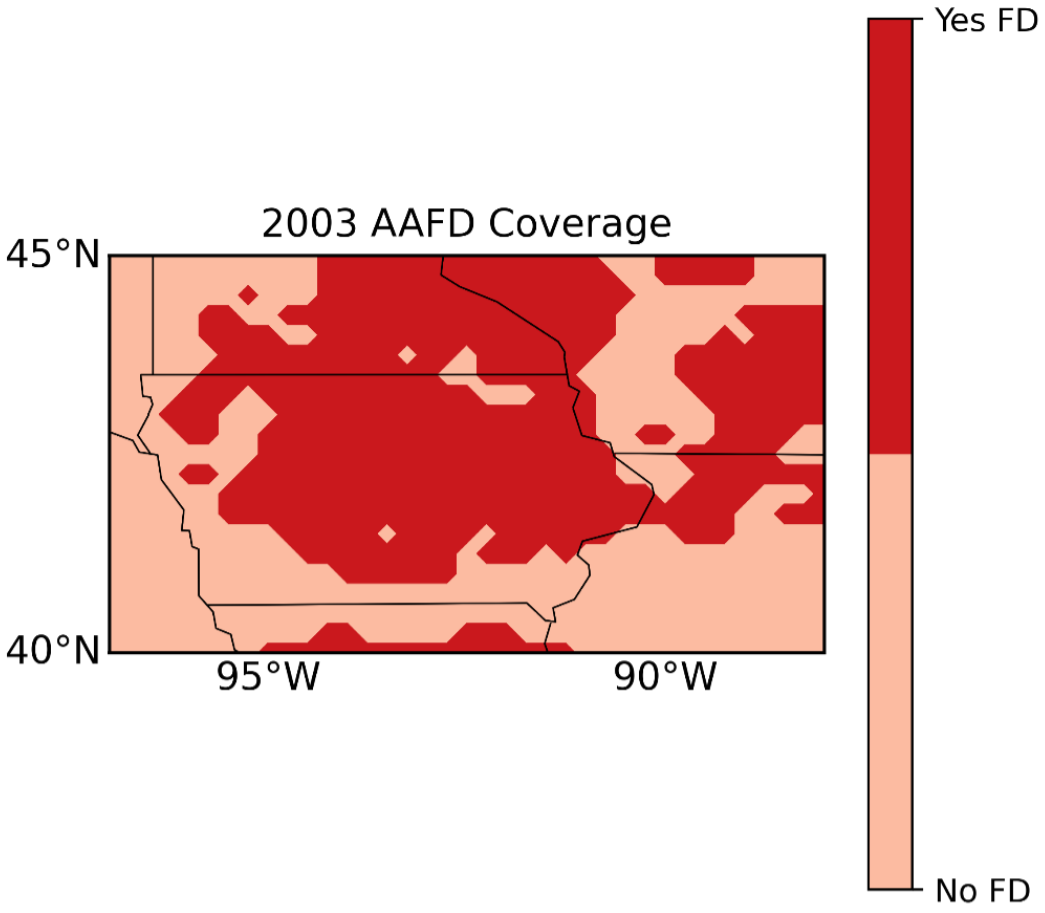

Figure A.5: Aerial coverage of the Midwest domain which underwent flash drought development during the AAFD which started on July 25, 2003.

Event #	Year	Month	Day	Strength	Peak Coverage at Pentad 0 (thousands of km^2)	Event coverage (9 pentads, thousands of km^2)
1	1982	7	10	-0.226	51.8	249.3
2	1983	6	10	-0.292	171.7	339.8
3	1984	6	20	-0.253	64.1	105.6
4	1985	5	21	-0.273	50.6	95.9
5	1987	9	3	-0.261	63.2	132.3
6	1988	9	28	-0.256	59.3	92.2
7	1989	2	20	-0.211	69.6	96.4
8	1989	9	8	-0.27	75.7	193.6
9	1992	9	3	-0.252	124.4	225.8
10	1995	7	25	-0.283	57.3	145.2
11	1995	9	23	-0.286	61.7	110.3
12	1998	5	16	-0.263	99.1	175.9
13	1999	10	3	-0.268	104.4	209.7
14	2000	4	1	-0.271	70.2	167.3
15	2002	2	15	-0.241	75	213.5
16	2003	6	15	-0.285	155.4	289.8
17	2004	4	21	-0.278	152	258.7
18	2005	2	20	-0.213	58.2	97.7
19	2005	6	20	-0.244	63.2	75.9
20	2005	10	18	-0.196	53.9	120.9
21	2006	5	6	-0.223	154.3	195.9
22	2008	10	28	-0.222	144.7	251.9
23	2010	7	15	-0.277	52	98.7
24	2012	4	11	-0.274	154.3	264
25	2012	10	13	-0.252	77.2	134.4
26	2013	4	16	-0.216	73.2	129.7
27	2013	7	30	-0.226	58.2	114.8
28	2014	2	15	-0.169	48	115.1
29	2016	9	13	-0.252	55.7	105.1
30	2017	10	8	-0.237	41.1	99.3
31	2020	3	22	-0.253	62.9	169.2
32	2020	5	1	-0.189	41.6	90.1

Table A.1: AAFD events across the SGP region.

Event #	Year	Month	Day	Strength	Peak Coverage at Pentad 0 (thousands of km^2)	Event coverage (9 pentads, thousands of km^2)
1	1981	2	20	-0.247	112.1	184.1
2	1981	4	16	-0.232	49.2	116.5
3	1982	3	17	-0.255	42.6	113.9
4	1985	3	27	-0.215	43.4	125.1
5	1987	4	1	-0.263	267.3	307
6	1991	6	5	-0.231	58	146.4
7	1992	4	21	-0.235	64	213.8
8	1994	5	1	-0.151	54	125.4
9	1999	10	3	-0.255	58.6	110.8
10	2001	5	31	-0.329	73.6	119.2
11	2002	10	23	-0.241	125	301.4
12	2003	7	25	-0.285	210.8	258.3
13	2004	8	24	-0.233	62.7	117.2
14	2006	5	1	-0.22	104.5	202
15	2007	4	16	-0.216	62.9	111.8
16	2011	8	24	-0.207	41.1	133.5
17	2012	5	1	-0.215	132.5	229.7
18	2013	6	20	-0.219	74.4	121.4
19	2014	7	5	-0.27	52	100.9
20	2015	2	25	-0.268	107.4	156.6
21	2016	5	11	-0.277	67.8	95.4
22	2017	5	11	-0.274	91.4	164.5
23	2019	6	25	-0.248	41.4	97.9

Table A.2: AAFD events across the Midwest region.

Winter La Niña Periods
1983-1984, 1984-1985 ,1988-1989, 1995-1996, 1998-1999, 1999-2000, 2000-2001, 2005-2006, 2007-2008, 2008-2009, 2010-2011, 2011-2012, 2016-2017, 2017-2018

Table A.3: Winter La Nina periods defined within this study.